Chemico-Biological Interactions 351 (2022) 109690

Contents lists available at ScienceDirect

Chemico-Biological Interactions

journal homepage: www.elsevier.com/locate/chembioint

Investigation of the antileishmanial activity and mechanisms of action of acetyl-thiohydantoins

Bruna Taciane da Silva Bortoleti [a,b], Manoela Daiele Gonçalves [c], Fernanda Tomiotto-Pellissier [a,b], Priscila Goes Camargo [e], João Paulo Assolini [b], Virginia Marcia Concato [b], Mariana Barbosa Detoni [b], Danielle Larazin Bidóia [b], Marcelle de Lima Ferreira Bispo [f], Camilo Henrique da Silva Lima [d], Fernando Cesar de Macedo Jr. [e], Ivete Conchon-Costa [b], Milena Menegazzo Miranda-Sapla [b], Pryscilla Fanini Wowk [g,*], Wander Rogério Pavanelli [b,**]

[a] Biosciences and Biotechnology Postgraduate Program, Carlos Chagas Institute, (ICC/Fiocruz/PR), Curitiba, Paraná, Brazil
[b] State University of Londrina (UEL/PR), Laboratory of Immunoparasitology, Londrina, Paraná, Brazil
[c] State University of Londrina (UEL/PR), Laboratory of Biotransformation and Phytochemistry, Londrina, Paraná, Brazil
[d] Federal University of Rio de Janeiro, Chemistry Institute, Rio de Janeiro, Brazil
[e] State University of Londrina (UEL/PR), Laboratory of Research on Bioactive Molecules, Londrina, Paraná, Brazil
[f] State University of Londrina (UEL/PR), Laboratory of Synthesis of Medicinal Molecules, Londrina, Paraná, Brazil
[g] Carlos Chagas Institute (ICC/Fiocruz/PR), Curitiba, Paraná, Brazil

ARTICLE INFO

Keywords:
Apoptosis-like
Heterocyclic
Molecular docking
L. amazonensis
Thiohydantoins

ABSTRACT

The currently available treatment options for leishmaniasis are associated with high costs, severe side effects, and high toxicity. In previous studies, thiohydantoins demonstrated some pharmacological activities and were shown to be potential hit compounds with antileishmanial properties.

The present study further explored the antileishmanial effect of acetyl-thiohydantoins against *Leishmania amazonensis* and determined the main processes involved in parasite death. We observed that compared to thiohydantoin nuclei, acetyl-thiohydantoin treatment inhibited the proliferation of promastigotes. This treatment caused alterations in cell cycle progression and parasite size and caused morphological and ultrastructural changes. We then investigated the mechanisms involved in the death of the protozoan; there was an increase in ROS production, phosphatidylserine exposure, and plasma membrane permeabilization and a loss of mitochondrial membrane potential, resulting in an accumulation of lipid bodies and the formation of autophagic vacuoles on these parasites and confirming an apoptosis-like process. In intracellular amastigotes, selected acetyl-thiohydantoins reduced the percentage of infected macrophages and the number of amastigotes/macrophages by increasing ROS production and reducing TNF-α levels. Moreover, thiohydantoins did not induce cytotoxicity in murine macrophages (J774A.1), human monocytes (THP-1), or sheep erythrocytes. *In silico* and *in vitro* analyses showed that acetyl-thiohydantoins exerted *in vitro* antileishmanial effects on *L. amazonensis* promastigotes in apoptosis-like and amastigote forms by inducing ROS production and reducing TNF-α levels, indicating that they are good candidates for drug discovery studies in leishmaniasis treatment. Additionally, we carried out molecular docking analyses of acetyl-thiohydantoins on two important targets of *Leishmania amazonensis*: arginase and TNF-alpha converting enzyme. The results suggested that the acetyl groups in the N1-position of the thiohydantoin ring and the ring itself could be pharmacophoric groups due to their affinity for binding amino acid residues at the active site of both enzymes via hydrogen bond interactions. These results demonstrate that thiohydantoins are promising hit compounds that could be used as antileishmanial agents.

* Corresponding author. Instituto Carlos Chagas – ICC/Fiocruz-PR, Prof. Algacyr Munhoz Mader, 3775, CEP 81350-010, Curitiba, Paraná, Brazil.
** Corresponding author. Universidade Estadual de Londrina – UEL-PR, Rodovia Celso Garcia Cid, PR-445 Km-380, CEP, 86057-970, Londrina, Paraná, Brazil.
E-mail addresses: pryscilla.wowk@fiocruz.br (P.F. Wowk), wanderpavanelli@uel.br (W.R. Pavanelli).

https://doi.org/10.1016/j.cbi.2021.109690
Received 26 January 2021; Received in revised form 28 September 2021; Accepted 7 October 2021
Available online 9 October 2021

1. Introduction

According to the World Health Organization (WHO), neglected tropical diseases cause more than one billion human deaths annually worldwide [1]. Leishmaniasis is a parasitic infection caused by protozoan parasites of the genus *Leishmania.* Leishmaniasis is considered an important neglected disease and is endemic in 90 tropical countries, where 13 million people are infected; it is closely associated with poverty and has a very large impact on human health [2]. Leishmaniasis has different clinical manifestations, with symptoms varying from cutaneous lesions to fatal visceral forms [1]. *Leishmania amazonensis* is the main species that causes American Tegumentary Leishmaniasis (ATL), which leads to severe forms of cutaneous leishmaniasis, specifically localized, mucocutaneous, disseminated or diffuse forms, and possesses high epidemiological and medical importance [3].

The current treatment for leishmaniasis involves antileishmanial drugs, such as amphotericin B, pentavalent antimonials, pentamidine, paromomycin, and miltefosine, but these drugs have several disadvantages, such as high cost, long-term treatment, severe side effects, and toxicity, which can lead to mortality [3]. Due to difficulties in treating leishmaniasis, novel efficient, low cost, and safe alternatives for antileishmaniasis therapies are greatly needed. The efficacy of several synthetic compounds has been investigated in the treatment of this disease [4–6].

In this context, thiohydantoins have emerged as an important class of compounds since they have a wide range of biological activities, such as fungicidal [7], antimutagenic [8], anticancer [9], antihypertensive [10], antibacterial [11], antiviral [12], antimicrobial [13] and anti-inflammatory [9]. Regarding the antiparasitic activity of thiohydantoins, previous *in vitro* studies demonstrated their activity against *Trypanosoma brucei* [14], *Plasmodium falciparum* [15], *L. donovani* [16] and *L. amazonensis* [17]. Their efficacy was also demonstrated in an acute mouse model of trypanosomiasis [14].

In our ongoing search to discover new antileishmanial agents, we evaluated the antileishmanial activity of twelve thiohydantoins (**Ia-l**) derived from amino acids [18] that demonstrated promising results, showing IC_{50} and SI values ranging from 9.31 to 10.4 μM and 3.9 to 5.3, respectively. These findings encouraged us to synthesize and investigate the antileishmanial potential of a series of acetyl-thiohydantoins (**1a-e**), aiming to verify the influence of the acetyl group at the N1-position of the thiohydantoin ring on the biological activity. After a preliminary screening with the promastigote forms of *L. amazonensis*, we performed other specific biological assays to elucidate the mechanisms of parasite death in the presence of the most active compounds. Based on these results, we chose two molecular targets, arginase (ARG) and TNF-alpha converting enzyme (TACE), to perform molecular docking studies in order to analyze the possible molecular interactions between our ligands and these important targets.

2. Materials and methods

2.1. General procedure for the synthesis of acetyl-thiohydantoins (1a-e)

Ammonium thiocyanate (13.3 mmol) and L-amino acids (13.3 mmol) were placed in a round-bottomed flask, and then, acetic anhydride (79.3 mmol) was added; the mixture was incubated at 100 °C for 30 min under magnetic stirring. After the solution cooled to room temperature, cold water (20 mL) was added, and the final solution was stored at 5 °C for one day. The formed crystals were removed by vacuum filtration, and the crude product was purified by recrystallization in water [13].

2.2. Nuclear magnetic resonance (NMR) of acetyl-thiohydantoins (1a-e)

1-Acetyl-5-propanamide-2-thioxoimidazolidin-4-one (1a): Yield 106.48 mg (43%); white solid; Mp 220–222 °C; ^{1}H NMR (400.13 MHz, DMSO-d_6) δ 1.91–2.34 (m, 4H), 2.70 (s, 3H), 4.77 (dd, J_1 = 2.15, J_2 = 6.10 Hz, 1H), 7.32 (s, 1H), 12.66 (s, 1H); ^{13}C NMR (100.61 MHz, DMSO-d_6) δ 25.31 (CH_3), 27.77 (CH_2), 29.18 (CH_2), 62.48 (CH), 170.27 (C═O), 172.99 (C═O), 173.54 (C═O), and 183.05 (C═S).

1-Acetyl-5-isobutyl-2-thioxoimidazolidin-4-one (1b): Yield 255.93 mg (90%); white solid; Mp 125–127 °C; ^{1}H NMR (400.13 MHz, DMSO-d_6) δ 0.85 (dd, J_1 = 6.12, J_2 = 8.06 Hz, 6H), 1.69–1.91 (m, 3H), 2.71 (s, 3H), 4.71 (dd, J_1 = 3.04, J_2 = 8.01 Hz, 1H), 12.65 (s, 1H); ^{13}C NMR (100.61 MHz, DMSO-d_6) δ 22.42 (CH_3), 23.60 (CH_3), 24.23 (CH_2), 27.80 (CH), 61.84 (CH), 170.20 (C═O), 174.06 (C═O), and 183.00 (C═S).

1-Acetyl-5-(2-(methylthio)ethyl)-2-thioxoimidazolidin-4-one (1c): Yield 261.66 mg (85%); white solid; Mp 93–94 °C; ^{1}H NMR (400.13 MHz, DMSO-d_6) δ 2.01 (s, 3H), 2.50 (br, 4H), 2.72 (s, 3H), 4.81 (d, J = 3.60 Hz, 1H), 12.67 (s, 1H); ^{13}C NMR (100.61 MHz, DMSO-d_6) δ 14.87 (CH_3), 27.83 (CH_3), 28.09 (CH_2), 28.56 (CH_2), 61.99 (C), 170.47 (C═O), 173.55 (C═O), and 183.12 (C═S).

1-Acetyl-5-((benzyl)methyl)-2-thioxoimidazolidin-4-one (1d): Yield 234.00 mg (70%); white solid; Mp 160–162 °C; ^{1}H NMR (400.13 MHz, DMSO-d_6) δ 2.70 (s, 3H), 3.13 (dd, J_1 = 2.67, J_2 = 13.90 Hz, 1H), 3.38 (dd, J_1 = 5.93, J_2 = 13.90 Hz, 1H), 5.00 (dd, J_1 = 2.67, J_2 = 5.93 Hz, 1H), 6.97–6.99 (m, 2H), 7.23–7.30 (m, 3H), 12.43 (s, 1H); ^{13}C NMR (100.61 MHz, DMSO-d_6) δ 27.80 (CH_3), 34.90 (CH_2), 63.98 (CH), 127.73 (CH), 128.91 (CH), 129.71 (CH), 134.63 (CH), 170.49 (C═O), 173.02 (C═O), and 182.78 (C═S).

1-Acetyl-5-((1H-indol-3-yl)methyl)-2-thioxoimidazolidin-4-one (1e): Yield 218.68 mg (57%); yellow solid; Mp 163–165 °C; ^{1}H NMR (400.13 MHz, DMSO-d_6) δ 2.68 (s, 3H), 3.33 (dd, J_1 = 2.51, J_2 = 14.78 Hz, 2H), 3.55 (dd, J_1 = 5.63, J_2 = 14.78 Hz, 1H), 4.99 (dd, J_1 = 2.56, J_2 = 5.52 Hz, 1H), 6.95–7.08 (m, 3H), 7.35 (dd, J_1 = 7.67, J_2 = 16.32 Hz, 2H), 10.97 (s, 1H), 12.30 (s, 1H); ^{13}C NMR (100.61 MHz, DMSO-d_6) δ 27.93 (CH_3), 64.14 (CH_2), 106.78 (CH), 111.91 (CH), 118.46 (CH), 119.09 (CH), 121.49 (CH), 124.62, 127.80 (C), 136.31 (C), 170.54 (C═O), 173.67 (C═O), and 182.92 (C═S).

2.3. Culture of Leishmania (Leishmania) amazonensis

Promastigote forms of *L. (L.) amazonensis* (MHOM/BR/1989/166MJO) were maintained in culture medium 199 (Gibco, Invitrogen, New York, USA) supplemented with 10% fetal bovine serum FBS (Gibco), 1 M HEPES buffer, 1% human urine, 1% L-glutamine, streptomycin and penicillin (Gibco), and 10% sodium bicarbonate. The parasites were maintained in B.O.D. at 24 °C in 25-cm^2 culture flasks. All the experiments were performed with the promastigote forms in the stationary growth phase (five-day culture).

2.4. Experimental animals

BALB/c mice weighing 20–25 g and aged 6–12 weeks were obtained from Carlos Chagas Institute/Fiocruz-PR, Curitiba, Brazil. The mice were maintained under sterile conditions in a controlled and disinfected environment and provided with sterile water, food, and shavings. Animals were used according to a protocol approved by the Ethics Committee for the Use of Animals of the State University of Londrina (24299.2017.66), to generate bone marrow-derived macrophages (BMDMs).

2.5. Murine macrophage and human monocyte cultures

J774A.1 murine macrophages (TIB-67; ATCC, Manassas, VA, USA) and bone marrow-derived macrophages (BMDMs), generated as previously described [19], were used as murine macrophages. To evaluate human monocytes, THP-1 cells (TIB-202; ATCC, Manassas, VA, USA) were used. J774 and THP-1 cells were grown in RPMI 1640 medium, and BMDMs were grown in DMEM supplemented with 1% L-glutamine, 10% sodium bicarbonate, 10% FBS, 10 U/ml penicillin, and 10 μg/ml streptomycin (Gibco). The cells were maintained in an incubator (37 °C,

5% CO_2) in 25-cm^2 culture flasks.

2.6. Viability of murine macrophages and human monocytes

To evaluate whether thiohydantoins affect the viability of THP-1 human monocytes, J774A.1 murine macrophages or BMDMs, an MTT assay was performed as described in Ref. [20]. THP-1 cells, BMDMs and J774A.1 cells (3×10^4 cells/ml) were incubated with thiohydantoins **I**, **1a**, **1b**, **1c**, **1d** and **1e** at concentrations of 2, 10, 20 and 40 μM for 24 h (37 °C, 5% CO_2) in 96-well plates. The cells were washed, and MTT (0.03 mg/ml) was added and incubated for 4 h. The MTT product (formazan crystals) was diluted with 100 μl of DMSO (Sigma-Aldrich, St Louis, MO, USA) and analyzed with a spectrophotometer (Thermo Fisher Scientific, Multiskan GO, Waltham, MA, USA) at 550 nm. The results are expressed as the percentage of viability compared to the control group according to the following formula: % (viable macrophages) = (treated thiohydantoins sample/sample untreated sample) OD x 100. The concentration that caused cytotoxicity in 50% of the cells (CC_{50}) of each cell line was calculated by nonlinear regression to the dose-response curve using GraphPad Prism 6.01 software. Cells cultures in RPMI or DMEM medium without treatment or with 0.1% DMSO (vehicle) were used as a negative control, and hydrogen peroxide (H_2O_2 0.4%) was used as a positive control.

2.7. Antipromastigote activity

For the initial screening, *L. amazonensis* promastigote forms (10^6 cells/ml) were treated with different thiohydantoins **I**, **1a**, **1b**, **1c**, **1d**, and **1e** at concentrations of 2, 10, 20, and 40 μM and maintained in a B.O.D. at 24 °C for 24 h. Subsequently, XTT solution was added, the samples were incubated at 25 °C for 2 h, and the samples were analyzed in a spectrophotometer at 450 nm. The concentration that inhibited 50% of parasites (IC_{50}) was calculated using GraphPad Prism software as previously described. For the selection of the best compounds, the selectivity index (CC_{50} J774/IC_{50}) was calculated. For the antiproliferative activity, promastigotes (10^6 cells/ml) were treated with thiohydantoin **I** and acetyl-thiohydantoins **1a** and **1e** at concentrations of 2.5, 5, and 10 μM, and then, the promastigotes were maintained in a B.O.D. at 24 °C. After 24, 48, and 72 h of treatment, viable parasites (determined by form and movement) were counted in a Neubauer chamber. M199 culture medium without treatment or with 0.1% DMSO (vehicle) was used as a negative control, and amphotericin B (AmB) (1 μM) was used as a positive control. The results are expressed as the percentage of reduction compared to the control group (considered 100%) according to the following formula: % (viable parasites) = (treated thiohydantoins parasites/control - untreated parasites) × 100.

2.8. Hemolytic assay

To assess erythrocyte viability, we performed a hemolytic assay. Blood was collected from sheep [Ethics Committee for animal experimentation of State University of Londrina: 82,862,016.60] with heparin, and the erythrocytes were washed three times with PBS (centrifugation at 1000 rpm for 10 min). A 2% erythrocyte suspension was prepared with PBS. Thiohydantoin **I** and acetyl-thiohydantoins **1a** and **1e** (2, 10, 20, and 40 μM) were incubated in a total volume of 200 μl with a 2% erythrocyte suspension (ratio of 1:1) in a 96-well plate for 3 h at 37 °C in 5% CO_2. PBS was used as a negative control, and Triton X was used as a hemolysis positive control. The plates were centrifuged at 1000 rpm for 10 min, and the supernatants were collected and analyzed by reading the absorbance at 550 nm.

2.9. Effects of thiohydantoins on Leishmania cell cycle progression

Analysis of the effect of thiohydantoin treatment on cell cycle progression was performed as previously described [21]. Promastigote forms (10^6 cells/ml) were treated with acetyl-thiohydantoins **1a** (IC_{50} 8 μM and 2x IC_{50} 16 μM) and **1e** (IC_{50} 6 μM and 2x IC_{50} 12 μM) for 24 h, and the parasites were subjected to centrifugation at 2000 RPM for 7 min and then resuspended in PBS. Subsequently, a binding buffer solution with 50 μg/ml propidium iodide (PI) was added and incubated for 30 min in the dark and on ice. The fluorescence of propidium iodide was estimated using a BD Accuri™ C6 Plus personal flow cytometer, and 10,000 events were collected. The DNA content was analyzed, and the percentages of parasites in different phases of the cycle (G0/G1, S, and G2/M) were determined.

2.10. Determination of parasite cell size

To determine parasite cell volume, promastigote forms (10^6 cells/ml) were untreated or treated with acetyl-thiohydantoins **1a** (IC_{50} 8 μM and 2x IC_{50} 16 μM) and **1e** (IC_{50} 6 μM and 2x IC_{50} 12 μM) and incubated for 24 h at 24 °C. Subsequently, the parasites were analyzed using a BD Accuri™ C6 Plus personal flow cytometer (BD Biosciences, San Jose, CA) [20,22]. Histograms were generated based on the forward scatter (FSC-A) parameter, which represents the cell size, and side scatter (SSC-A), which represents the complexity of the cells. A total of 10,000 events were acquired in the region corresponding to the parasites. Vehicle (DMSO 0.1%) was used as a negative control.

2.11. Morphological and ultrastructural analyses of promastigotes by scanning electron microscopy (SEM) and transmission electron microscopy (TEM)

SEM was performed to analyze morphological changes in cell surface topography. *L. amazonensis* promastigotes (10^6 parasites/mL) were treated with acetyl-thiohydantoins **1a** (IC_{50} 8 μM and 2x IC_{50} 16 μM) and **1e** (IC_{50} 6 μM and 2x IC_{50} 12 μM) for 24 h at 25 °C. After the treatment, the parasites were fixed with 2.5% glutaraldehyde in 0.1 M sodium cacodylate buffer and allowed to adhere to coverslips coated with poly-L-lysine for 60 min. Then, the parasites were dehydrated with increasing ethanol concentrations (30–100%), subjected to a critical point drying (Baltec SCD-030), and coated with gold for visualization with a high-resolution FEI SCIOS double-beam electron microscope.

To evaluate the ultrastructural changes in the acetyl-thiohydantoin-treated parasites by TEM, the promastigotes were treated and fixed as described above. Then, the samples were postfixed with 1% OsO_4, 0.8% potassium ferrocyanide, and 10.0 mM $CaCl_2$ in 0.1 M sodium cacodylate buffer for 1 h at room temperature in the dark. The samples were washed in 0.1 M sodium cacodylate buffer and dehydrated with increasing concentrations of acetone (50–100%). The entire acetone content was gradually replaced with EPON™ epoxy resin by cell diffusion, and after 72 h at 60 °C, the resin was polymerized. Nanoscale slices (60–70 nm) were cut with an ultramicrotome (PowerTomer BMC - Germany) and contrasted with 5% uranyl acetate and 2% lead citrate. Finally, the samples were analyzed on a JEOL USA JEM 1400 transmission electron microscope. *L. amazonensis* promastigotes maintained in M199 culture medium without treatment or with 0.01% DMSO (vehicle) were used as negative controls.

2.12. Reactive oxygen species (ROS) generation in promastigotes and infected macrophages

ROS generation was evaluated by the conversion of nonfluorescent H_2DCFDA to the highly fluorescent 2′,7′-dichlorofluorescein (DCF) in *L. amazonensis* promastigote forms (10^6 cells/ml) treated with acetyl-thiohydantoins **1a** (IC_{50} 8 μM and 2x IC_{50} 16 μM) and **1e** (IC_{50} 6 μM and 2x IC_{50} 12 μM) and infected macrophages treated with **1a** (IC_{50} 8 μM and 2x IC_{50} 16 μM) and **1e** (IC_{50} 6 μM and 2x IC_{50} 12 μM) as described [20]. Untreated parasites and infected cells were used as a negative control, and H_2O_2 (0.4%) was used as a positive control. ROS production was measured with excitation/emission wavelengths of 488/530 nm on

a fluorescence microplate reader (Victor X3, PerkinElmer, Turku, Finland).

2.13. Determination of mitochondrial membrane potential

To determine the mitochondrial membrane potential, promastigote forms (10^6 cells/ml) were treated for 24 h with acetyl-thiohydantoins **1a** (IC_{50} 8 μM and 2x IC_{50} 16 μM) and **1e** (IC_{50} 6 μM and 2x IC_{50} 12 μM) at 24 °C. Tetramethyl rhodamine ethyl ester (TMRE) (Sigma, St. Louis, MO, USA) staining was used to assess the inner mitochondrial membrane potential, according to Ref. [22]. Untreated parasites were used as a negative control, and carbonyl cyanide 3-chlorophenylhydrazone (CCCP) was used as a positive control. The results were analyzed at excitation/emission wavelengths of 480/580 nm on a fluorescence microplate reader (Victor X3).

2.14. Determination of phosphatidylserine exposure and cellular membrane integrity

Promastigotes (10^6 cells/ml) were treated with acetyl-thiohydantoins **1a** (IC_{50} 8 μM and 2x IC_{50} 16 μM) and **1e** (IC_{50} 6 μM and 2x IC_{50} 12 μM) for 24 h at 24 °C, phosphatidylserine exposure was detected using Annexin-V FITC (Invitrogen, Eugene, USA), and cellular membrane integrity was detected with propidium iodide (PI) (0.50 μg/ml) (Sigma, St. Louis, MO, USA) [20]. Data acquisition was performed at excitation/emission wavelengths of 488/520 nm for Annexin-V and excitation/emission wavelengths of 480/580 nm for PI on a fluorescence microplate reader (Victor X3).

2.15. Detection of lipid body accumulation

To determine lipid body accumulation, promastigotes of *L. amazonensis* (10^6 cells/ml) were treated with acetyl-thiohydantoins **1a** (IC_{50} 8 μM and 2x IC_{50} 16 μM) and **1e** (IC_{50} 6 μM and 2x IC_{50} 12 μM) for 24 h. Subsequently, parasites were labeled with 10 μg/mL Nile red (Sigma-Aldrich, St. Louis, MO, USA) for 30 min [23] and analyzed in a Perkin-Elmer Victor X3 Fluorimeter using wavelengths of 530 nm and 635 nm for excitation and emission, respectively. Untreated parasites were used as a negative control, and PBS treatment was used as a positive control.

2.16. Quantification of autophagic vacuoles

To evaluate lipid body accumulation, promastigote forms (10^6 cells/ml) treated for 24 h with acetyl-thiohydantoins **1a** (IC_{50} 8 μM and 2x IC_{50} 16 μM) and **1e** (IC_{50} 6 μM and 2x IC_{50} 12 μM) were labeled with monodanzilcadaverine (MDC, 50 μM; Sigma-Aldrich, St. Louis, MO, USA) for 1 h at 24 °C [24] and analyzed on a Perkin-Elmer Victor X3 Fluorimeter using wavelengths of 380 nm and 525 nm for excitation and emission, respectively. Untreated parasites were used as a negative control, and PBS treatment was used as a positive control.

2.17. Antiamastigote assay

To evaluate the percentage of infected macrophages and the number of amastigotes/macrophages, an antiamastigote assay was performed as previously described by Refs. [22,25]. J774 macrophages (10^5 cells/ml) were infected with *L. amazonensis* promastigotes (10^6 parasites/ml) overnight. After infection, the noninternalized promastigotes were removed, and the infected cells were treated with acetyl-thiohydantoins **1a** and **1e** (IC_{50} and 2x IC_{50}), DMEM (negative control), 1 μM AmB (positive control), and 0.1% DMSO (vehicle) for 24 h (37 °C, 5% CO_2). Subsequently, the cells were stained with Giemsa (Laborclin, Pines-PR Brazil), and 20 fields were analyzed by optical microscopy (Olympus BX41, Olympus Optical Co., Ltd., Tokyo, Japan) (1000x magnification) to determine the percentage (%) of infected macrophages and the number of amastigotes per macrophage.

2.18. Determination of nitrite as an estimate of NO levels and TNF-α measurement

Nitric oxide (NO) levels in antiamastigote assay supernatants were determined through the Griess method according to Refs. [22,25]. The supernatants of the antiamastigote assay were used to measure cytokine tumor necrosis factor-alpha (TNF-α) levels by enzyme-linked immunosorbent assay (ELISA) according to the manufacturer's instructions (eBiosciences®, USA). Plates were read at 450 nm using an ELISA plate reader (Thermo Scientific, Multiskan GO).

2.19. Statistical analysis

The data are expressed as the mean ± standard error of the mean (SEM). Three independent experiments were performed, each with duplicate datasets. The data were analyzed using GraphPad Prism statistical software (GraphPad Software, Inc., USA, 500.288). Significant differences between the groups were determined through *t*-test and one-way ANOVA followed by Tukey's test for multiple comparisons. Differences were considered statistically significant when $p \leq 0.05$.

2.20. In silico study of thiohydantoins by molinspiration and admetSAR analyses

For the *in silico* study, the structures of thiohydantoin **I** and acetyl-thiohydantoins **1a** and **1e** were analyzed with the *Molinspiration* Property Calculator program (www.molinspiration.com), and the parameters related to oral bioavailability were determined according to Lipinski's rule of five (Ro5) [26] followed by the additional rule proposed [27]. In addition, we analyzed the pharmacological parameters of thiohydantoins through the online database admetSAR (http://lmmd.ecust.edu.cn/admetsar1) [28].

2.21. Molecular modeling

2.21.1. Preparation of proteins and ligands

The structural model of arginase from *L. amazonensis* was constructed by homology modeling using the crystal structure of arginase from *Leishmania mexicana* as a template [29] (PDB ID: 4ITY, resolution: 1.95 Å) as described by Ref. [17]. TNF-α converting enzyme from *Homo sapiens* was selected from the Protein Data Bank (PDB) (Code: 3L0V, Resolution: 1.75 Å) [17]. The 3D structures of acetyl-thiohydantoins (**1a** and **1e**) were constructed in ChemDraw, and geometry optimization was performed using the MM2 force field implemented in ChemBio3D v.12.0 (PerkinElmer Informatics) [30].

2.21.2. Molecular docking Procedures

Molecular docking was performed using GOLD v. 2020.1 (Genetic Optimization for Ligand Docking) applying the ChemPLP scoring function [31]. The hydrogen atoms were added to the proteins based on ionization inferred by the program, and other parameters were set to default. For ARG, we performed clustering analysis to identify the probable best-scored pose results [32]. The ligands were subjected to 50 iterative runs, and the binding site was point centered between manganese ions at x: 15.141, y: 15.125, z: 5.40, within a 25 Å radius. For TACE, the method was validated by redocking with root-mean-square deviation (RMSD) calculation pose result <2.00 Å [33]. The ligands were subjected to 10 iterative runs. The region of interest was centered on atomic zinc metal in the active site at x: 9.103 y: 12.706, z: 24.147, with a 12 Å radius. The analysis of intermolecular interactions for both targets was carried out using Discovery Studio Visualizer (Dassault Systèmes BIOVIA, Discovery Studio Modeling Environment, Release 2017, San Diego: Dassault Systèmes, 2016).

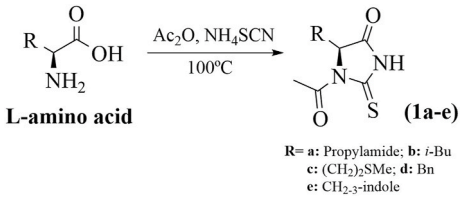

Scheme 1. Synthetic route for preparation of acyl-thiohydantoins (**1a-e**).

3. Results

3.1. Chemistry

The synthesis and characterization of thiohydantoin **I** (derivative of the amino acid glycine) were reported previously by Ref. [13]. Here, this compound was used as a control to compare the influence of the acetyl group in the N1-position of the heterocyclic ring. In addition, five acetyl-thiohydantoins (**1a-e**) were synthesized (Schemes 1 and 2 and Table 1) by treatment of the corresponding L-amino acids (glutamine, leucine, methionine, phenylalanine, and tryptophan) with acetic anhydride and ammonium thiocyanate to produce the corresponding compounds with great yields of 43–90% [34].

Thiohydantoins **1b-c** derived from amino acids with nonpolar side chains showed the best yields (85–90%), followed by the phenylalanine derivative **1d** with a yield of 70%. Poor yields were observed for the tryptophan derivative **1e** and the glutamine derivative **1a**, which showed yields of 57 and 43%, respectively. All detected ^{1}H and ^{13}C NMR signals were compared with data published in the literature. The ^{1}H NMR spectra showed the characteristic signal for the NH proton at 12.3–12.7 ppm, and the ^{13}C NMR spectra showed the signals for C=O and C=S endocyclic carbon resonances at 172.9–174.3 and 179.1–183.1 ppm, respectively. The signals corresponding to the CH_3 protons and C=O of the acyl group were observed at 2.68–2.71 ppm in the ^{1}H NMR spectra and at 156.76–170.54 ppm in the ^{13}C NMR spectra, respectively. Furthermore, the other signals were consistent with the presence of the corresponding aliphatic or aromatic group in each compound of the series.

3.2. Thiohydantoins cause low cytotoxicity in monocytes, murine macrophages, and erythrocytes

We investigated whether treatment with thiohydantoin nuclei (compound **I**) and five acetyl-thiohydantoins (**1a-e**) alters the viability of human monocytes, murine macrophages, and sheep erythrocytes by MTT assay and hemolytic test. The CC_{50} of thiohydantoins ranged between 27 and > 40 μM for THP-1 cells, 30.5–37 μM for BMDMs, and 30–36 μM for J774 cells (Table 2). In addition, in the hemolytic assay,

Table 1
Results for the synthesis of acyl-thiohydantoins (**1a-e**).

L-amino acid	Thiohydantoin	Radical	Yield (%)
Glutamine	**1a**	Propylamide	43
Leucine	**1b**	Isobutil	90
Methionine	**1c**	$(CH_2)_2SCH_3$	85
Phenylalanine	**1d**	Benzyl	70
Tryptophan	**1e**	CH_2-3-indole	57

Table 2
CC_{50} in THP-1, BMDM, and J774; IC_{50} in promastigote forms and Thiohydantoin selectivity index.

Thiohydantoins	THP-1 CC_{50} μM (±SEM)	BMDM CC_{50} μM (±SEM)	J774 CC_{50} μM (±SEM)	Promastigotes IC_{50} μM (±SEM)	SI μM (±SEM)
I	28 (±0.08)	31 (±0.06)	30 (±0.02)	ND	ND
1a	30 (±0.12)	34 (±0.09)	32 (±0.02)	8 (±0.05)	4
1b	32 (±0.04)	34 (±0.12)	31 (±0.01)	12 (±0.11)	2.58
1c	>40 (±0.90)	31 (±0.04)	33 (±0.01)	15 (±0.08)	2.20
1d	33 (0.02)	30.50 (±0.03)	34 (±0.09)	11.50 (±0.23)	2.95
1e	27 (±0.13)	37 (±0.04)	36 (±0.01)	6 (±0.06)	6

Human leukemic monocytes (THP-1), murine bone marrow-derived macrophages (BMDM), murine macrophages (J774) (3×10^4) and promastigotes forms (*L. amazonensis*) (1×10^6) were treated with different thiohydantoins **I**, **1a**, **1b**, **1c**, **1d** and **1e** (2, 10, 20, 40 μM) for 24 h and analyzed by MTT or XTT assays. CC_{50}: Cytotoxic concentration for 50% of cells, IC_{50}: 50% inhibitory concentration of parasites, SI: Selectivity index, where CC_{50} J774/IC_{50}, ND: Not determined. The values represent the mean ± SEM of three independent experiments performed in duplicate.

Table 3
Thiohydantoin hemolytic assay.

	% Hemolysis (±SEM)		
Concentration (μM)	I	1a	1e
2	NH	NH	NH
10	NH	NH	NH
20	0.2 (±0.09)	0.1 (±0.12)	0.1 (±0.08)
40	0.3 (±0.11)	0.2 (±0.11)	0.3 (±0.15)

NH: non hemolytic.

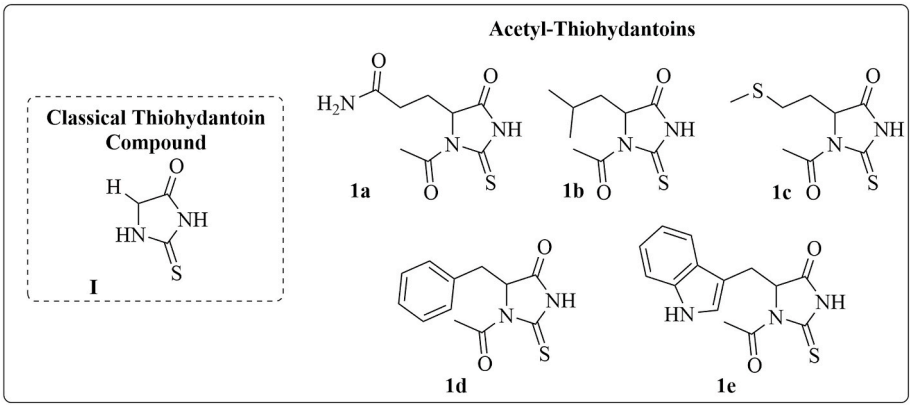

Scheme 2. Structure of acetyl-thiohydantoins compounds **1a** and **2c-g**.

Table 4
Molinspiration bioactivity score data of the Thiohydantoins.

Thiohydantoins	Melting point	Veber's Rules			Lipinski's Rules				
		H-Acc + H-Don (≤12)	RB (≤10)	tPSA (≤140°Å^2)	MW (g.mol^{-1}) (≤500)	miLog P (≤5)	nON (≤10)	nOHNH (≤5)	N° Violations
I	204-206 °C	5	0	41.12	116.14	−0.53	3	2	0
1a	220-222 °C	9	3	92.50	229.26	−1.66	6	3	0
1e	196.2–204.8 °C	7	2	65.20	287.34	1.02	5	2	0

MW: molecular weight; Log P: Log of partition-coefficient; H-Acc/nON: number of Hydrogen bond acceptor; H-Don/nOHNH: number of Hydrogen bond donor; RB: number of rotatable bonds; tPSA: molecular polar surface area.

Table 5
Prediction of pharmacological parameters evaluation of Thiohydantoin using the admetSAR toolbox.

ADMET Properties	I	1a	1e	References
Carcinogenicity	N	N	N	Lagunin et al., 2009
AMES toxicity	N	N	N	Hansen et al., 2009
Human intestinal absortion	H	H	H	Shen et al., 2010
Caco-2 permeability	H	H	H	Pham The et al., 2011
Blood-brain barrier penetration	Y	Y	Y	Shen et al., 2010
Predicted aqueous solubility	Y	Y	Y	Wang et al., 2007
hERG inhibition	N	N	N	Marchese Robinson et al., 2011
CYP2C9 Inhibitor	N	N	N	Cheng et al., 2011
CYP2D6 Inhibitor	N	N	N	Cheng et al., 2011
CYP3A4 Inhibitor	N	N	Y	Cheng et al., 2011
CYP1A2 Inhibitor	N	N	Y	Cheng et al., 2011
CYP2C19 Inhibitor	N	N	N	Cheng et al., 2011
CYP inhibitory promiscuity	L	L	H	Cheng et al., 2011

Predictions based on: admetSAR online database developed by Cheng et al., 2012.
N: No; H: High; Y: Yes; L: Low.

the thiohydantoins with higher selective indexes, **1a** (SI 4), **1e** (SI 6) and nucleus **I**, which were selected for comparison, did not cause hemolysis (NH - nonhemolytic) at 2 and 10 μM, while at 20 and 40 μM, they showed 0.1–0.3% hemolysis on average (Table 3); these low values confirm the low toxicity of the compounds.

3.3. Calculation of the drug similarity of thiohydantoins

A molecule that has the potential to be an oral drug generally follows Ro5+Veber rules. Thiohydantoins **I**, **1a,** and **1e** satisfied the rules with no violations, indicating the likelihood that they are good drug candidates (Table 4), and they showed good hydrophilicity/lipophilicity ratios with adequate intestinal absorption, demonstrating bioavailability and metabolic stability. Additionally, according to the admetSAR rules, thiohydantoins **I**, **1a,** and **1e** are neither carcinogenic nor mutagenic, have high intestinal absorption, permeate Caco-2 cells, penetrate the blood-brain barrier, have high solubility, are not hERG inhibitors and are not inhibitors of cytochrome P450 isoforms (Table 5).

3.4. Thiohydantoins exert a leishmanicidal effect on promastigote forms

We investigated the direct effect of the thiohydantoin nucleus (**I**) and 5 acetyl-thiohydantoins against promastigote forms of *L. amazonensis* for 24 h. The thiohydantoin nucleus (**I**) did not show leishmanicidal activity within 24 h, although acetylation at the N1-position of the ring and modification of the side chains (position C5) contributed to potential activity because of the observed leishmanicidal effect on all modified thiohydantoins. Lower IC_{50} values were obtained for acetyl-thiohydantoins **1e** (IC_{50} 6 μM ± 0.05) and **1a** (IC_{50} 8 μM ± 0.05), followed by acetyl-thiohydantoins **1d** (11.50 μM ± 0.23), **1b** (12 μM ± 0.11) and **1c** (15 μM ± 0.08) (Table 2). We selected thiohydantoin derivatives with higher selective indexes: **1a** (SI = 4) and **1e** (SI = 6). The thiohydantoin nucleus (**I**) was selected for the comparison of antiproliferative promastigote activity. We observed that **I** did not show leishmanicidal activity in 24 h compared to the control (untreated parasites), so **I** was not chosen for experiments, even though it inhibited more than 50% of parasites in 48 h and 72 h at 2.5 μM, 5 μM, and 10 μM ($p \leq 0.0001$) (Fig. 1A). Thiohydantoin **1a** treatment for 24 h at a concentration of 10 μM was able to reduce parasite numbers by 60% ($p \leq 0.001$), and after 48 h, treatment with concentrations of 2.5 μM, 5 μM and 10 μM reduced parasite numbers by more than 50%, while at 72 h, we observed that concentrations of 2.5, 5 and 10 μM caused reductions of 42.86%, 51.24% and 63.06%, respectively ($p \leq 0.0001$) (Fig. 1B). Finally, thiohydantoin **1e** at concentrations of at 5 and 10 μM reduced parasite numbers by 46% and 65% in 24 h, respectively ($p < 0.01$). At 48 h, concentrations of 2.5, 5 and 10 μM caused decreases in promastigote numbers of 53.25%, 58% and 68.43% ($p < 0.0001$), respectively, and at 72 h, we observed that treatment with 2.5, 5 and 10 μM caused reductions of 41.88%, 47.3%, 48.77% ($p < 0.0001$), respectively (Fig. 1C). Vehicle (DMSO 0.1%) exerted no leishmanicidal effect at any time tested, and AmB (1 μM), as a positive control, inhibited 100% (±0.0) of *L. amazonensis*.

3.5. Acetyl-thiohydantoins induce cell cycle arrest at the G2/M phase in promastigotes

Cell cycle analysis by flow cytometry indicated that promastigotes treated with acetyl-thiohydantoins **1a** (IC_{50} 8 μM and 2x IC_{50} 16 μM) presented decreases in the subpopulations of cells in the G0/G1 phase and increases in the subpopulations of cells in the S and G2/M phases (Fig. 2B) compared to the control (untreated parasites) (Fig. 2A) ($p \leq 0.0001$). Furthermore, the population of cells in the sub-G0 phase was not increased by thiohydantoin treatment. **1e** (IC_{50} 6 μM and 2x IC_{50} 12 μM) increased number of cells in the G0/G1 and S phases and decreased the numbers of cells in the G2/M phase ($p \leq 0.0001$) (Fig. 2C) compared to the control (untreated parasites) (Fig. 2A).

3.6. Acetyl-thiohydantoins reduce the cell volume of promastigote forms

After 24 h of treatment with acetyl-thiohydantoins **1a** (IC_{50} 8 μM and 2x IC_{50} 16 μM) and **1e** (IC_{50} 6 μM and 2x IC_{50} 12 μM), we observed a reduction in the cell volume of parasites in relation to the control (untreated parasites) according to flow cytometer analysis (Fig. 3A and B), and these results were statistically significantly different ($p \leq 0.0001$).

3.7. Acetyl-thiohydantoins induce morphological and ultrastructural changes in promastigotes

SEM and TEM were performed to determine the morphological (Fig. 4) and ultrastructural (Fig. 5) changes, respectively, induced by thiohydantoin treatment in promastigotes. Untreated parasites (Fig. 4A, B, 5A, 5B) and vehicle-treated parasites (0.1% DMSO) (Fig. 4C, D, 5C, 5D) exhibited normal characteristics, such as elongated bodies, flagella proportional to body size, smooth and intact cell surfaces, and well-preserved structures. However, promastigotes treated with acetyl-thiohydantoins **1a** and **1e** at the IC_{50} and 2x the IC_{50} showed morphological and ultrastructural changes, such as rounded shapes, reduced cell

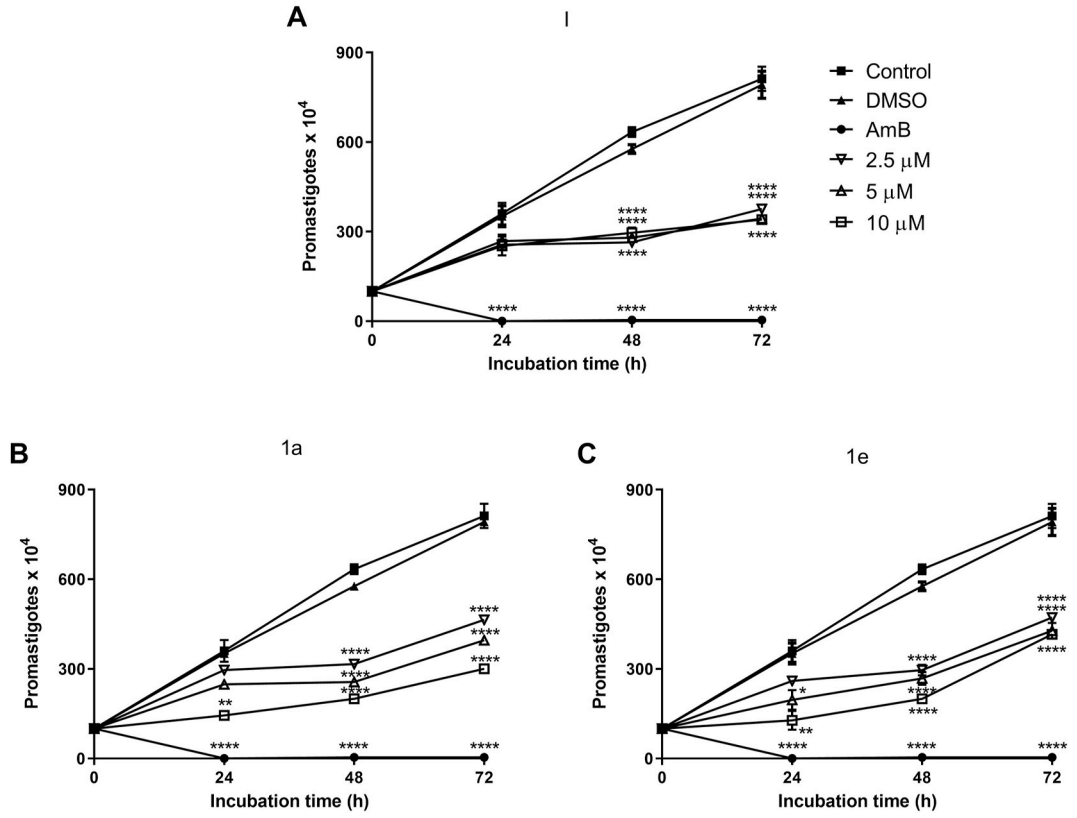

Fig. 1. Antiproliferative effect caused by thiohydantoins on *L. amazonensis* promastigotes. Promastigote forms of *L. amazonensis* were treated with different thiohydantoin compounds A) **I**, B) **1a** and C) **1e** (2.5, 5 and 10 μM), negative control (medium 199), vehicle control (0.1% DMSO), and positive control (amphoterecin B [AmB], 1 μM), and parasite proliferation was evaluated at 0, 24, 48 and 72 h. The values represent the mean ± SEM of three independent experiments performed in duplicate. * Significant difference compared to the control group ($p \leq 0.05$), ** ($p < 0.005$), **** ($p \leq 0.0001$).

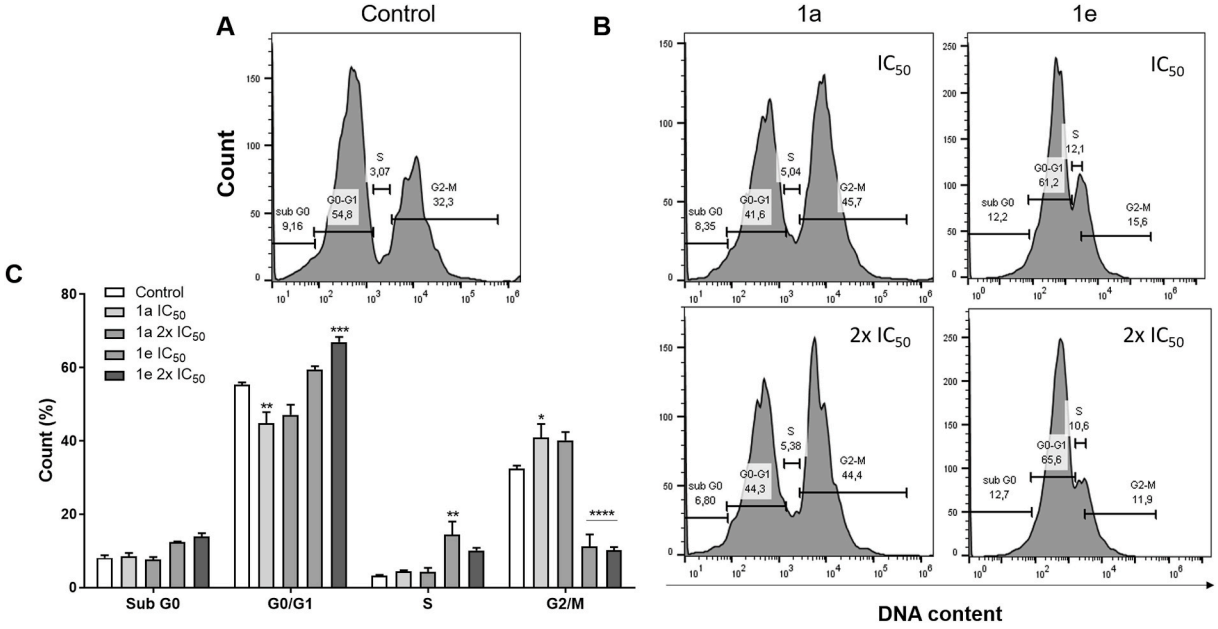

Fig. 2. Effect of acetyl-thiohydantoins on *L. amazonensis* cell cycle progression. Cell cycle distribution of *L. amazonensis* promastigotes after treatment with acetyl-thiohydantoins **1a** (IC_{50} and 2x IC_{50}) and **1e** (IC_{50} and 2x IC_{50}) for 24 h was analyzed by flow cytometry with representative histograms showing DNA content plotted against cell numbers (B). Medium 199 was used as the control (A). Quantitative analysis of promastigotes at different stages of the cell cycle was performed (C). The values represent the mean ± SEM of three independent experiments performed in duplicate. * Significant difference compared to the control group ($p \leq 0.05$), ** ($p \leq 0.01$).

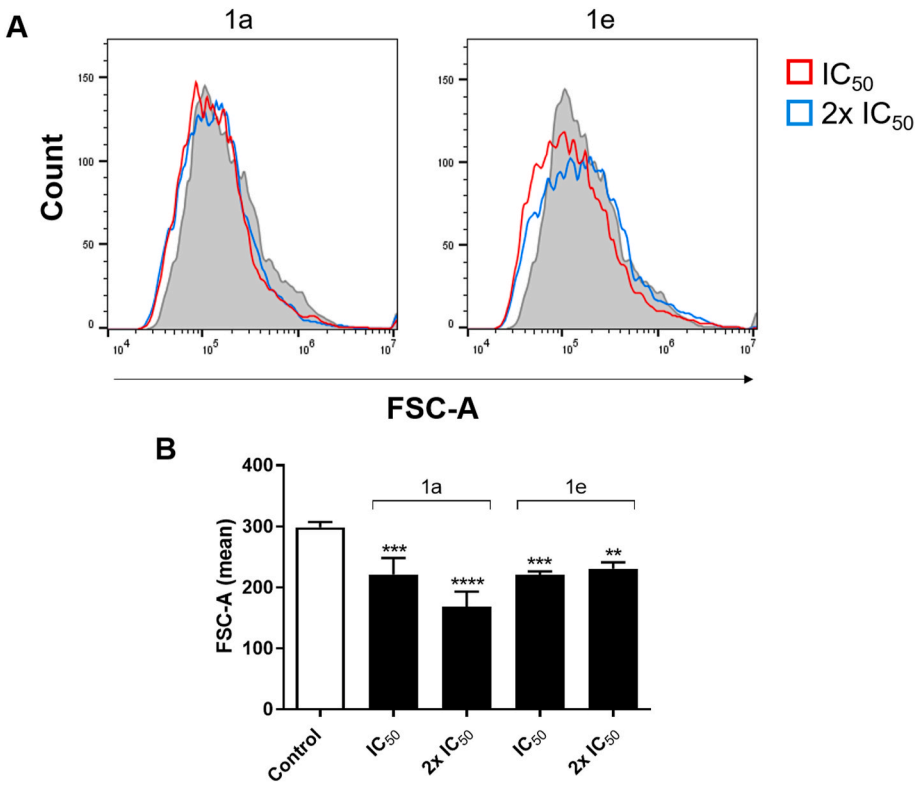

Fig. 3. Cell size of *L. amazonensis* promastigote forms after acetyl-thiohydantoin treatment for 24 h. *L. amazonensis*-promastigote forms treated with **1a** (IC_{50} 8 μM and 2x IC_{50} 16 μM) and **1e** (IC_{50} 6 μM and 2x IC_{50} 12 μM) (A) and quantitative analysis of cell volume (B). FSC-A was considered a function of cell size. The black line corresponds to the control (untreated parasites), and the red and blue areas indicate the parasites treated with IC_{50} and 2x IC_{50}. Representative histograms of at least three independent experiments are shown. The values represent the mean ± SEM of three independent experiments performed in duplicate. ** Significant difference compared to the control group ($p \leq 0.01$), *** ($p \leq 0.001$), **** ($p \leq 0.0001$). (For interpretation of the references to colour in this figure legend, the reader is referred to the Web version of this article.)

body size, cell surface roughness, plasma membrane damage, cytoplasmic content leakage (Fig. 4E–T), intense accumulation of lipid-storage bodies, more autophagic vacuoles, mitochondrial swelling, and multiple flagella and nuclei (Fig. 5E-X).

3.8. Acetyl-thiohydantoins induce an increase in reactive oxygen species production, a loss of mitochondrial integrity, a loss of phosphatidylserine exposure, and a loss of plasma membrane integrity in promastigotes

The direct effect of acetyl-thiohydantoins on *L. amazonensis* promastigote forms was observed, and we then decided to explore the mechanism involved in parasite elimination. After treatment of parasites with acetyl-thiohydantoins **1a** (IC_{50} 8 μM and 2x IC_{50} 16 μM) and **1e** (IC_{50} 6 μM and 2x IC_{50} 12 μM), we observed an increase in ROS generation (Fig. 6A) ($p \leq 0.01$) and a loss of mitochondrial integrity through decreased TMRE fluorescence intensity (Fig. 7B) ($p \leq 0.0001$) in relation to the control. Additionally, it was demonstrated that the treated parasites exhibited increased staining with annexin V (Fig. 6C) and PI (Fig. 6D) ($p \leq 0.0001$) compared to the control parasites.

3.9. Acetyl-thiohydantoins induce lipid body and autophagic vacuole formation in promastigotes

Promastigote forms treated with acetyl-thiohydantoins **1a** (IC_{50} 8 μM and 2x IC_{50} 16 μM) and **1e** (IC_{50} 6 μM and 2x IC_{50} 12 μM) revealed the increased presence of lipid bodies in relation to the control through staining with Nile red, a fluorescent dye with a high affinity for neutral lipids, demonstrating that thiohydantoins induce lipid body accumulation in parasites (Fig. 7A) ($p \leq 0.0001$). MDC is a fluorescent probe that accumulates in autophagic vacuoles, and acetyl-thiohydantoins **1a** (IC_{50} 8 μM and 2x IC_{50} 16 μM) and **1e** (IC_{50} 6 μM and 2x IC_{50} 12 μM) increased the intensity of MDC fluorescence in relation to the control (Fig. 7B) ($p \leq 0.05$).

3.10. Acetyl-thiohydantoins exert leishmanicidal activity on intracellular amastigotes

To determine whether acetyl-thiohydantoins have a leishmanicidal effect on *L. amazonensis*-infected macrophages, we performed an anti-amastigote assay. Our results showed that 24 h post infection, the control and DMSO groups consisted of 75.33% (±4.00) and 75.66% (±3.00) infected macrophages, respectively, which indicates that the groups did not differ from each other. Acetyl-thiohydantoin **1a** treatment at IC_{50} and 2x IC_{50} resulted in 12.09% (±1.00) and 7.17% (±0.59) infected macrophages, representing reductions of 63.24% (±1.00) and 68.16% (±0.59), while treatment with **1e** resulted in 17.86% (±0.44) and 7.88% (±0.65) infected cells, representing reductions of 57.47% (±0.44) and 67.45 (±0.65) compared to the controls, respectively (Fig. 8A). In addition, the number of amastigotes per macrophage in the control and DMSO groups was 1.71 (±0.05) and 1.67 (±0.05), and it was also reduced by acetyl-thiohydantoin **1a** treatment at IC_{50} and 2x IC_{50} by 0.93 (54.40% ± 0.01) and 0.81 (47.40% ± 0.02), while **1e** treatment reduced these numbers by 1.21 (70.76% ± 0.01) and 0.93 (54.40% ± 0.01) (Fig. 8B) in relation to the controls, respectively. Interestingly, our data showed that the effect of **1a** and **1e** treatment at 2x IC_{50} had effects similar to those of AmB (positive control) in terms of the percentage of infected cells.

3.11. Acetyl-thiohydantoins did not alter NO levels but induced ROS production and reduced TNF-α levels in L. amazonensis-infected macrophages

To verify the production of the main microbicidal molecules and cytokines produced by macrophages, we assessed the levels of nitrite (as an indirect estimate of NO production), ROS and TNF-α. Our results showed that infected macrophages treated with **1a** (IC_{50} 8 μM and 2x IC_{50} 16 μM) and **1e** (IC_{50} 6 μM and 2x IC_{50} 12 μM) did not exhibit altered NO levels (Fig. 9A) but exhibited increased ROS production (Fig. 9B) ($p \leq 0.0001$) and reduced TNF-α levels compared to the control (Fig. 9C)

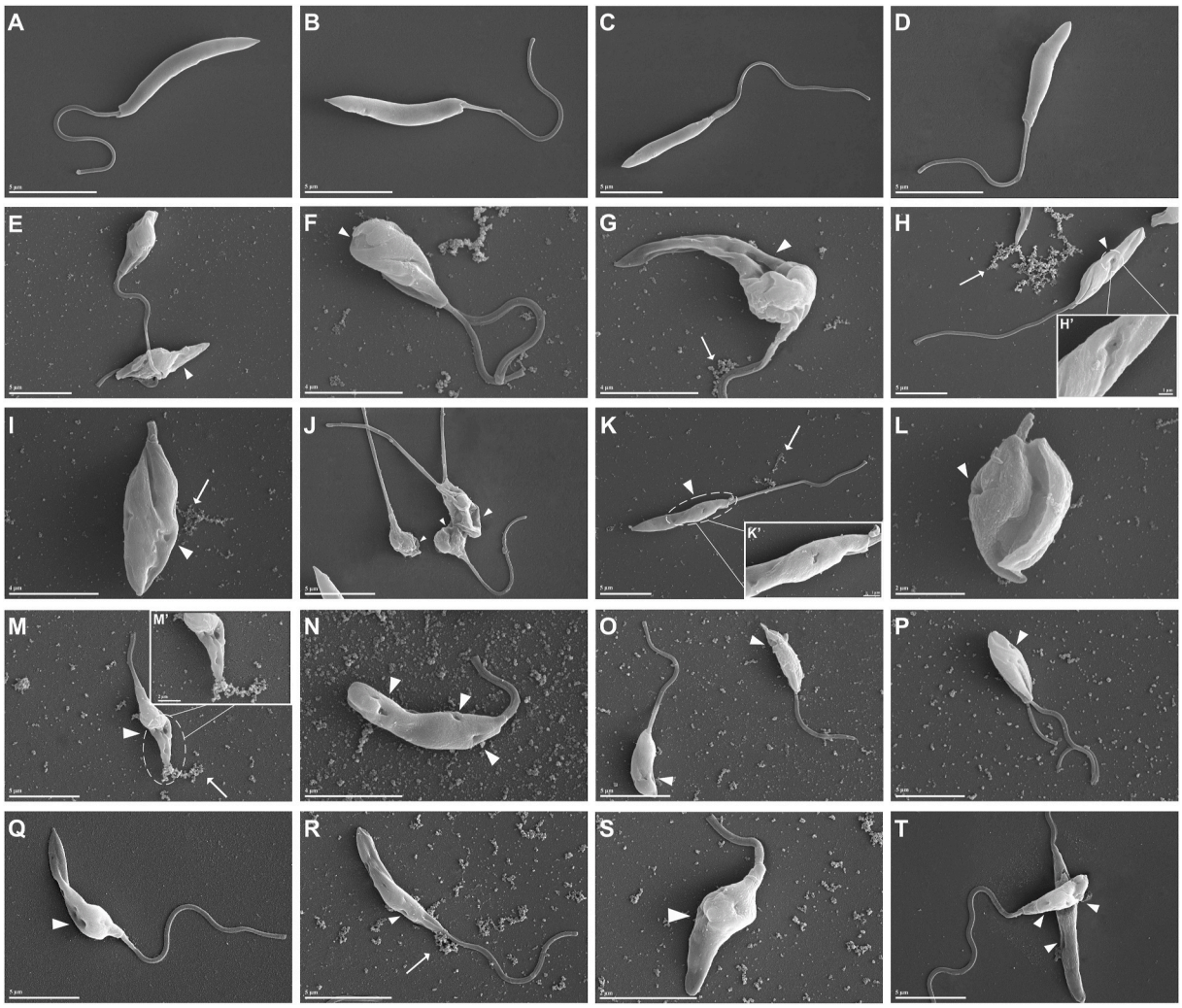

Fig. 4. Morphological alterations of promastigotes of *L. amazonensis* treated with IC_{50} and 2x IC_{50} of **1a** and **1e** for 24 h, analyzed by scanning electron microscopy (SEM). (A, B) Untreated promastigotes; (C, D) promastigotes treated with vehicle (DMSO 0.01%); (E–H) promastigotes treated with IC_{50} of **1a**; (I–L) promastigotes treated with 2x IC_{50} of **1a**; (M–P) promastigotes treated with IC_{50} of **1e**; (Q–T) promastigotes treated with 2x IC_{50} of **1e**. (white arrow) Leakage of cytoplasmic contents, (white arrowhead) plasma membrane damage. Scale bars = 5 μm (A-E, H, J, K, M, O-R, and T), 4 μm (F, G, I, and N), 2 μm (L, M′, and S) and 1 μm (H′ and K′).

($p \leq 0.01$).

3.12. Acetyl-thiohydantoin molecular docking studies

Clustering analysis of the docking simulation of the ARG ligand complexes (**1a** and **1e**) showed the best pose results, common hydrogen-bonding interactions of the compounds mainly with Asp141 and His154 residues, and coordination with the metal Mn^{2+} at 2.46 Å (Fig. 10A and B). The redocking simulation of the TACE complex with its cocrystallized hydantoin ligand exhibited an RMSD value = 0.58. The docking results for compounds **1a** and **1e** showed common hydrogen-bonding interactions mainly with His405, His409 and His415, which are described as important residues in the active site, and showed coordination with the Zn^{2+} metal at 1.67–2.54 Å (Fig. 11A-C).

4. Discussion

The current pharmacotherapy for leishmaniasis presents some limitations due to its high toxicity, poor tolerability, difficult administration, systemic side effects and high cost [3]. Additionally, treatments have become less effective due to increasing drug resistance. Moreover, there are no efficient vaccines against leishmaniasis [35,36].

Thiohydantoin is a synthetic and heterocyclic compound that presents microbicidal properties and potential characteristics and has become a candidate for drug development [37]. *In silico* studies demonstrated that acetyl-thiohydantoins present good intestinal absorption, metabolic stability, and bioavailability according to Lipinski's and Veber's rules [26,27]. Furthermore, the molecules are not carcinogenic or mutagenic according to the admetSAR rules [28], and thus, they have a high probability of being good drug candidates since poor ADMET properties are one of the reasons drug candidates fail during clinical trials [38].

Previous studies demonstrated that thiohydantoins did not present cytotoxicity in J774 [16], HepG2 [39], and Vero [40] cells. Our findings showed a similar effect for the nucleus and the six acetyl-thiohydantoins, which did not alter the viability of bone marrow-derived macrophages (BMDMs) or murine macrophage (J774), and human monocyte (THP-1) cell lines and did not cause the hemolysis of ovine erythrocytes.

In the search for antileishmanial agents, we initially screened the nucleus and the five acetyl-thiohydantoins on promastigote forms. Our results showed that the nucleus (**I**) does not have an antipromastigote effect, and all acetyl-thiohydantoins were capable of inhibiting the proliferation of the promastigote forms of *L. amazonensis*, but only **1a**

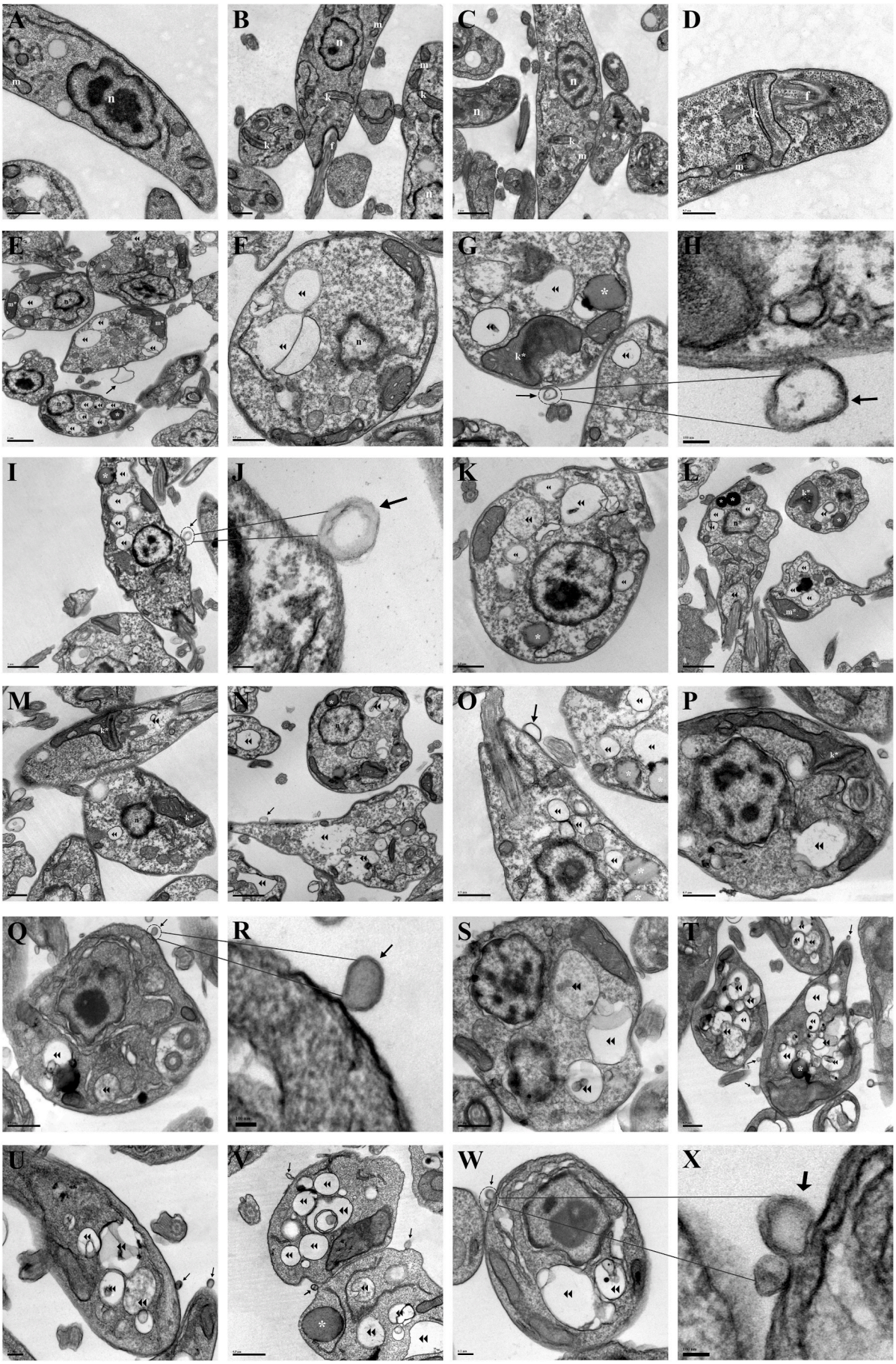

(caption on next page)

Fig. 5. Ultrastructural alterations of promastigotes of *L. amazonensis* treated with IC_{50} and 2x IC_{50} of **1a** and **1e** for 24 h, analyzed by transmission electron microscopy (TEM). (A, B) Untreated promastigotes; (C, D) promastigotes treated with vehicle (DMSO 0.01%); (E–J) promastigotes treated with IC_{50} of **1a**; (K–N) promastigotes treated with 2x IC_{50} of **1a**; (O–S) promastigotes treated with IC_{50} of **1e**; (T–X) promastigotes treated with 2x IC_{50} of **1e**. (f) flagellum; (k) kinetoplast; (k*) mitochondrial swelling in the kinetoplast region; (m) mitochondria; (m*) mitochondrial swelling; (n) nucleus; (n*) nuclear disorganization; (arrow) blebbing of plasma membrane; (*) lipid-storage bodies (⏭); autophagic vacuole. Scale bars = 1 μm (C, E, I, L, and N), 0.5 μm (A, B, D, F, G, K, M, O, P, Q, S, T, and V), 0.2 μm (U and W) and 100 nm (H, J, R, and X).

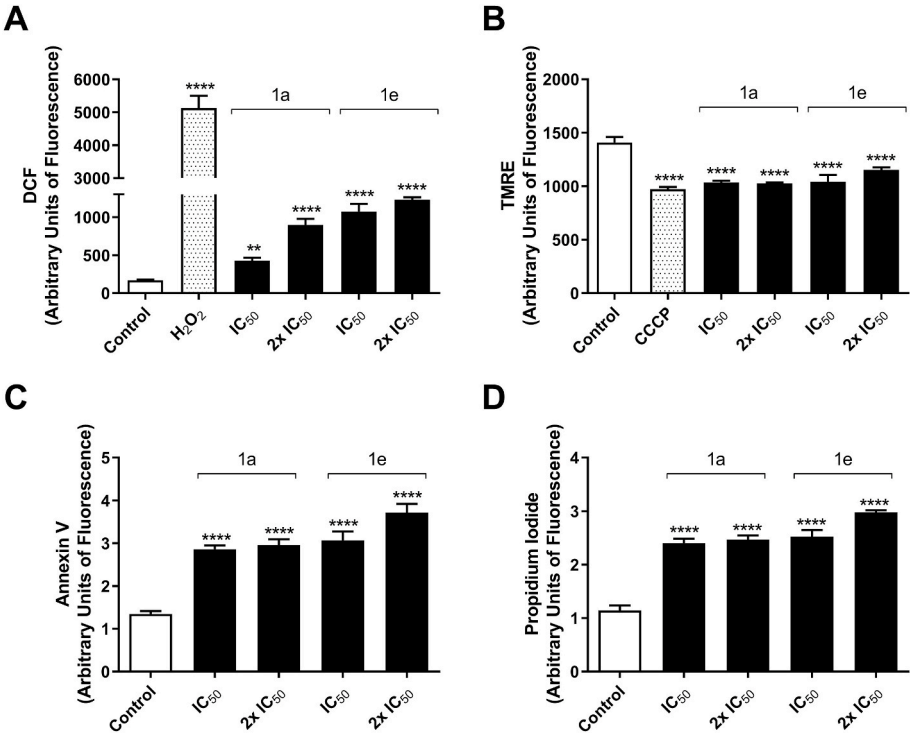

Fig. 6. Mechanism underlying the death of *L. amazonensis* promastigote forms induced by acetyl-thiohydantoins. Promastigote forms were treated or not for 24 h with thiohydantoins **1a** and **1e** (IC_{50} and 2x IC_{50}) and reactive oxygen species production was evaluated with a 2′,7′-dichlorofluorescein (DCF) probe (A), mitochondrial membrane integrity was evaluated by tetramethylrhodamine ethyl ester (TMRE) assay (B), phosphatidylserine exposure was evaluated by Annexin V labeling (C) and plasma membrane integrity was evaluated by propidium iodide staining (D). The data represent the mean ± SEM of three independent experiments performed in duplicate. ** Significant difference compared to the control ($p \leq 0.01$), **** ($p \leq 0.0001$). Untreated parasites were used as a negative control, and H_2O_2 and CCCP were used as positive controls for ROS and mitochondrial depolarization, respectively.

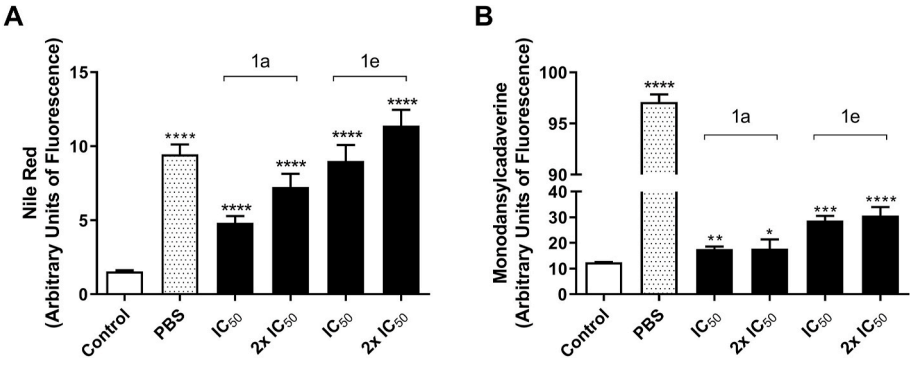

Fig. 7. Effect of thiohydantoins on lipid body accumulation and autophagic vacuole formation in *L. amazonensis* promastigote forms. Promastigote forms were treated for 24 h with thiohydantoins **1a** and **1e** (IC_{50} and 2x IC_{50}) and lipid body and autophagic vacuole formation was evaluated by labeling with Nile red (A) and monodansylcadaverine (B). Untreated parasites were used as a negative control, and PBS was used as a positive control. The data represent the mean ± SEM of three independent experiments performed in duplicate. * Significant difference compared to the control ($p \leq 0.05$), ** ($p \leq 0.01$), *** ($p \leq 0.001$), **** ($p \leq 0.0001$).

and **1e** had a good (high) selectivity index. Comparable effects were described against *T. brucei* [14], *P. falciparum* [15], *L. donovani* [16] and *L. amazonensis* [17]. Confirming these results, the cell cycle analysis demonstrated that thiohydantoin **1a** was capable of decreasing the subpopulation in the GO/G1 phase and increasing the subpopulation in the G2/M phase, negatively influencing the growth and DNA synthesis of parasites and resulting in deleterious effects on cytokinesis [41–43]. On the other hand, **1e** showed a different effect on the cell cycle, increasing the subpopulations in the GO/G1 and S phases and decreasing the subpopulation in the G2/M phase. With this alteration, the cells possess one copy of DNA, exhibit a reduction in DNA replication, and do not undergo DNA synthesis and mitosis. Similarly, cell cycle arrest at the G0/G1 phase has been correlated with apoptosis-like cell death [44], and similar effects on the cell cycle were observed with semicarbazone derivatives against *L. amazonensis* promastigotes (Cavalcanti de Queiroz et al., 2019) and salisylaldoxime and *trans*--dibenzalacetone against *L. donovani* promastigotes [45,46].

Additionally, we observed that acetyl-thiohydantoins **1a** and **1e** can reduce *L. amazonensis* promastigote cell size, leading to morphological and structural changes such as reduction in the cell body, damage and blebbing of the plasmatic membrane, leakage of cytoplasmic contents, mitochondrial dysfunction, irregular flagellation, and nuclear alterations. These events are characteristic of apoptosis, and similar effects were observed with other compounds [20,47].

In unicellular parasites, such as *Leishmania*, different types of cell death, including apoptosis, which is a form of programmed cell death that can control pathogen dissemination, occur [48]. In addition to microscopic analysis, biochemical methods were used to confirm this

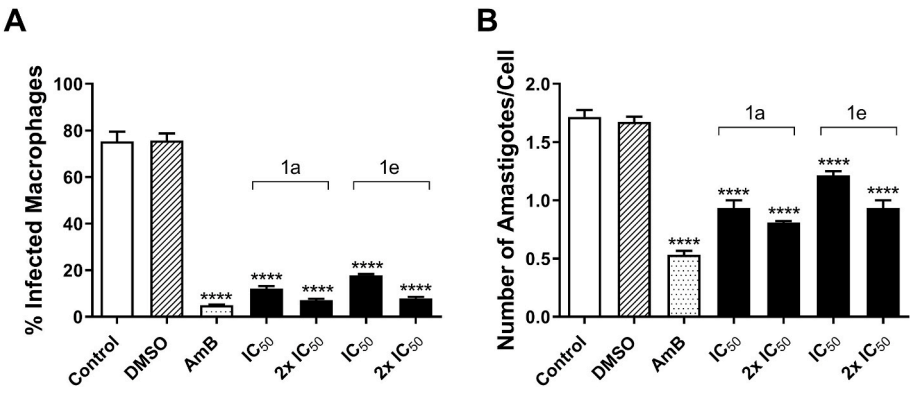

Fig. 8. Effect of acetyl-thiohydantoins on *L. amazonensis*-infected macrophages. *L. amazonensis*-infected macrophages were treated for 24 h with acetyl-thiohydantoins **1a** and **1e** (IC_{50} and 2x IC_{50}), and the percentage of infected macrophages (A) and the number of amastigotes per macrophage (B) were evaluated. Control (infected macrophages), DMSO 0.01% (vehicle) and 1 μM AmB (positive control) were included. The values represent the mean ± SEM of three independent experiments performed in duplicate. **** Significant difference compared to the control ($p \leq 0.0001$).

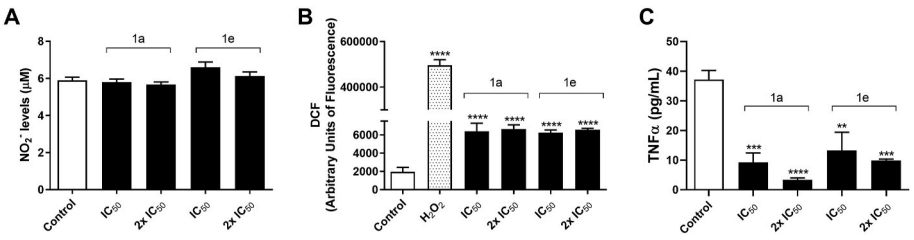

Fig. 9. NO and ROS production and TNF-α levels in *L. amazonensis*-infected macrophages treated with acetyl-thiohydantoins. Infected macrophages were subjected to 24 h of treatment with acetyl-thiohydantoins **1a** and **1e** (IC_{50} and 2x IC_{50}). A) The Griess method was used to evaluate the nitrite levels in the supernatants of cultured cells, B) the fluorescent probe DCF was used to measure the reactive oxygen species levels, and C) the TNF-α levels were measured by ELISA. H_2O_2 was used as a positive control for ROS production. The values represent the mean ± SEM of three independent experiments performed in duplicate. ** Significant difference compared to the control ($p \leq 0.01$), *** ($p \leq 0.001$), **** ($p \leq 0.0001$).

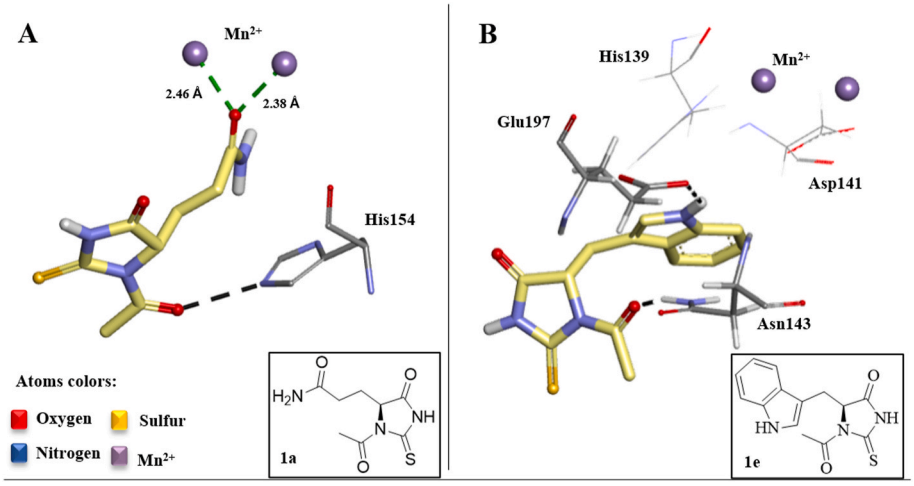

Fig. 10. Interaction diagrams of the docking pose results of acetyl-thiohydantoins **1a** (A) and **1e** (B) in the active site of ARG. Residues interacting via H-bonds are represented by sticks, and those interacting via hydrophobic interactions are represented by lines. The dashed black lines represent the H-bonding interactions with residues, and the metal coordination is shown as green lines. (For interpretation of the references to colour in this figure legend, the reader is referred to the Web version of this article.)

phenomenon. Thiohydantoins are capable of inducing ROS production and altering the plasma membrane and phosphatidylserine exposure in *L. amazonensis* promastigotes [17], and it was observed in our study that promastigotes treated with acetyl-thiohydantoin exhibited cell shrinkage, changes in the plasma membrane, phosphatidylserine exposure, and mitochondrial depolarization, which are classic apoptotic phenotypes. We also found an increase in ROS generation and mitochondrial depolarization in acetyl-thiohydantoin-treated parasites. ROS are formed during normal metabolism or are associated with the eradication of invading parasites. These molecules act on parasites, disrupting the unique parasite mitochondria, which defines their functionality, via oxidative phosphorylation. These events can lead to the execution of apoptosis [49], and one of the hallmarks of apoptosis, the dysfunction of mitochondria, causes cellular stress for parasite functions, resulting in lipid body formation [50–52]; this phenomenon was observed with acetyl-thiohydantoins **1a** and **1e** treatments.

Autophagy in trypanosomatids is a biological process involved in the maintenance of the parasite life cycle, removal of damaged cellular components and modulation of host immunity through the formation of structures named autophagic vacuoles; this process can be activated during cellular stress, which is caused by an increase in ROS production [53,54]. Acetyl-thiohydantoins were capable of increasing autophagic vacuole formation, as seen in the fluorimeter assay and TEM analyses, and the exacerbation of this autophagic pathway can also lead to regulated cell death in parasites [55].

Some pharmacological properties of synthetic compounds include antimicrobial, antioxidant, anticancer, anti-inflammatory, and antiparasite properties, making them important scaffolds in medicinal chemistry [37]. Acetyl-thiohydantoins **1a** and **1e** are effective against *L. amazonensis* amastigote forms by reducing the percentage of infected

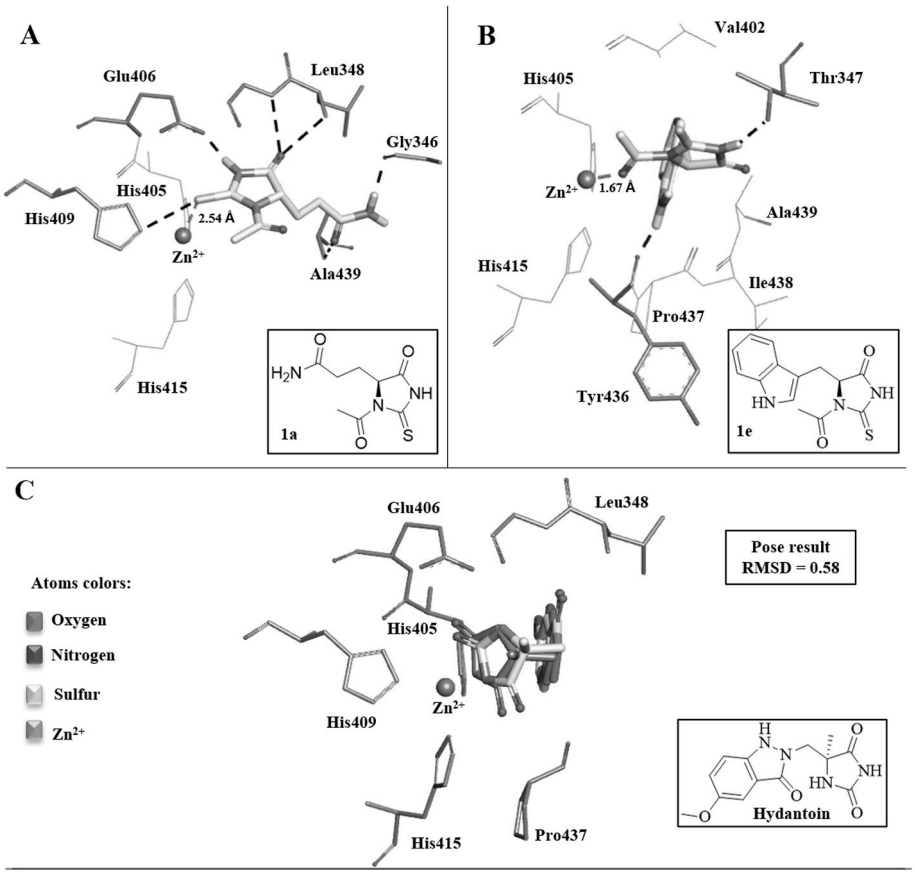

Fig. 11. Interaction diagrams of the docking pose results of (A) acetyl-thiohydantoin **1a**, (B) acetyl-thiohydantoin **1e** and (C) redocking (yellow) of the hydantoin cocrystallized ligand (gray) in the active site of TACE (PDB 3L0V). Residues interacting via H-bonds are represented by sticks, and those interacting via hydrophobic interactions are represented by lines. The dashed black lines represent the H-bonding interactions with residues, and the metal coordination is shown as green lines.

macrophages and the number of amastigotes/macrophages. Similar results were observed with other synthetic compounds, such as 4-aryloxy-7-chloroquinoline derivatives against *L. donovani* amastigotes [56], semicarbazone derivatives against *L. amazonensis* amastigotes (Cavalcanti de Queiroz et al., 2019), and 1,2-dioxanes against *L. donovani* amastigotes [57].

Acetyl-thiohydantoins **1a** and **1e** are capable of inducing the production of ROS, which are important microbicidal molecules produced by macrophages against pathogens such as *Leishmania*; ROS production culminates in parasite death via direct oxidative damage or via a variety of innate and adaptive mechanisms, resulting in infection resolution [58,59].

To obtain new insights into acetyl-thiohydantoin-induced ROS production, we performed molecular docking studies on arginase (ARG; E. C. 3.5.3.1, L-arginine aminohydrolase). ARG is a metalloenzyme expressed in *Leishmania* spp. that is involved in regulating the growth of the parasite, among other processes, due to its important role in the urea cycle (Garcia et al., 2019). Docking simulations of acetyl-thiohydantoins and ARG targets were previously described by our research group [17], so we decided to investigate whether the addition of an acetyl group in the N1 position of the thiohydantoin ring could contribute to the binding affinity of these compounds. We observed that the oxygen atom from the side chain of compound **1a** engaged in coordination with the Mn^{2+} ion, while the oxygen atom from the acetyl group contributed positively to hydrogen-bonding interactions with His154 (to **1a**), which is an important residue for enzyme stabilization during catalytic activity [17], and Asn143 (to **1e**). Our studies demonstrated that the **1a** and **1e** compounds are capable of binding to the active site of ARG, suggesting that they could inhibit this target.

TNF-α is an important proinflammatory cytokine that enhances the activity of macrophages, leading to a type 1 T helper (Th1) immune response, and microbicidal action is required to control infection by most *Leishmania* strains, leading to protection. On the other hand, TNF-α causes tissue damage and loss of splenic architecture in experimental VL and is associated with tissue pathology in CL [60–62]. Acetyl-thiohydantoins **1a** and **1e** reduced the TNF-α levels in *L. amazonensis*-infected macrophages and are related to anti-inflammatory effects [9]. Additionally, thiohydantoins belong to a class of compounds with a hydantoin substructure. Hydantoins have the capacity to inhibit TNF-α converting enzyme (TACE), a zinc metalloprotease of the ADAM family that blocks the formation of the soluble form (17 kDa) from the membrane-bound form (26 kDa) of TNF-α [37]. Some hydantoin compounds are TACE inhibitors that are able to act as effective anti-inflammatory drugs based on their ability to decrease levels of soluble TNF-α (17 kDa) [63,64].

Therefore, we also performed molecular docking studies on TACE (E. C. 3.4.24.86, ADAM 17 endopeptidase), which is a zinc metalloprotease of the ADAM family that blocks the formation of the soluble form (17 kDa) from the membrane-bound form (26 kDa) of TNF-α [37]. The docking results were successfully validated by redocking, showing an RMSD value of 0.58. The docking simulations for compounds **1a** and **1e** on TACE showed common hydrogen-bonding interactions, mainly with His405, His409 and His415, which are described as important residues in the active site [63], and the docking simulations showed coordination with metal Zn^{2+} at 1.67 Å by a sulfur atom from the thiohydantoin ring of **1a** and at 2.54 Å by an oxygen atom from the acetyl group of **1e**. Compound **1a** showed more hydrogen bonds in the binding site of TACE than **1e,** which in turn was closer to the Zn^{2+} ion (1.67 Å). This proximity could be explained by the interaction of the NH group of the imidazole ring present in the side chain of **1e** with the Tyr436 residue,

which contributed to this binding pose. Our studies demonstrated that **1a** and **1e** could bind to the active site of TACE, inhibiting this target and contributing to anti-inflammatory activity in conjunction with anti-leishmanial activity.

5. Conclusion

In conclusion, thiohydantoin analogs are more promising than nuclear thiohydantoin (**I**). Among the six thiohydantoins, two acetyl-thiohydantoins (**1a** and **1e**) exert a potential leishmanicidal effect on promastigote forms via an apoptosis-like mechanism, and in *L. amazonensis*-infected macrophages, these acetyl-thiohydantoins increased ROS production and decreased TNF-α levels, culminating in the elimination of intracellular parasites. These compounds have important characteristics and may be potential candidates for anti-*leishmaniasis* drug development.

Declaration of competing interest

The authors declare that they have no known competing financial interests or personal relationships that could have appeared to influence the work reported in this paper.

Acknowledgments

The authors gratefully acknowledge Dr. Juliano Bordignon, Dr. Iriane Egler, and Dr. Letusa Albrecht for the corrections and suggestions about this article. The authors would like to thank the Spectroscopy Laboratory (LABSPEC) NMR-UEL/FINEP for the NMR experiments and Wagner Nagib de Souza (ICC/Fiocruz-PR) for the final art of the graphical abstract.

Appendix A. Supplementary data

Supplementary data to this article can be found online at https://doi.org/10.1016/j.cbi.2021.109690.

Funding

WRP (301594/2018-0) is a CNPq fellow.

References

[1] WHO; World Health Organization, Leishmaniasis. https://www.who.int/news-room/fact-sheets/detail/leishmaniasis, 2019. (Accessed 13 September 2019) accessed.
[2] A.S. Nagle, S. Khare, A.B. Kumar, F. Supek, A. Buchynskyy, C.J.N. Mathison, N. K. Chennamaneni, N. Pendem, F.S. Buckner, M.H. Gelb, V. Molteni, Recent developments in drug discovery for leishmaniasis and human African trypanosomiasis, Chem. Rev. 114 (2014) 11305–11347, https://doi.org/10.1021/cr500365f.
[3] S. Sundar, J. Chakravarty, An update on pharmacotherapy for leishmaniasis, Expet Opin. Pharmacother. 16 (2015) 237–252, https://doi.org/10.1517/14656566.2015.973850.
[4] A. Cavalcanti de Queiroz, M.A. Alves, E.J. Barreiro, L.M. Lima, M.S. Alexandre-Moreira, Semicarbazone derivatives as promising therapeutic alternatives in leishmaniasis, Exp. Parasitol. 201 (2019) 57–66, https://doi.org/10.1016/j.exppara.2019.04.003.
[5] M. Ortalli, S. Varani, C. Rosso, A. Quintavalla, M. Lombardo, C. Trombini, Evaluation of synthetic substituted 1,2-dioxanes as novel agents against human leishmaniasis, Eur. J. Med. Chem. 170 (2019) 126–140, https://doi.org/10.1016/j.ejmech.2019.02.070.
[6] G. Serban, Future prospects in the treatment of parasitic diseases: 2-amino-1,3,4-Thiadiazoles in leishmaniasis, Molecules 24 (2019) 1557, https://doi.org/10.3390/molecules24081557.
[7] K. Kobyłka, G. Żuchowski, W. Tejchman, K.K. Zborowski, Synthesis, spectroscopy, and theoretical calculations of some 2-thiohydantoin derivatives as possible new fungicides, J. Mol. Model. 25 (2019) 268, https://doi.org/10.1007/s00894-019-4146-9.
[8] A. Takahashi, H. Matsuoka, Y. Ozawa, Y. Uda, Antimutagenic properties of 3,5-Disubstituted 2-thiohydantoins, J. Agric. Food Chem. 46 (1998) 5037–5042, https://doi.org/10.1021/JF980430X.
[9] K.R.A. Abdellatif, W.A.A. Fadaly, Y.A. Mostafa, D.M. Zaher, H.A. Omar, Thiohydantoin derivatives incorporating a pyrazole core: design, synthesis and biological evaluation as dual inhibitors of topoisomerase-I and cycloxygenase-2 with anti-cancer and anti-inflammatory activities, Bioorg. Chem. 91 (2019) 103132, https://doi.org/10.1016/j.bioorg.2019.103132.
[10] T. Dylag, M. Zygmunt, D. Maciag, J. Handzlik, M. Bednarski, B. Filipek, K. Kieć-Kononowicz, Synthesis and evaluation of in vivo activity of diphenylhydantoin basic derivatives, Eur. J. Med. Chem. 39 (2004) 1013–1027, https://doi.org/10.1016/J.EJMECH.2004.05.008.
[11] F. Fujisaki, K. Shoji, M. Shimodouzono, N. Kashige, F. Miake, K. Sumoto, Antibacterial activity of 5-Dialkylaminomethylhydantoins and related compounds, Chem. Pharm. Bull. (Tokyo). 58 (2010) 1123–1126, https://doi.org/10.1248/cpb.58.1123.
[12] A.M.S. El-Sharief, Z. Moussa, Synthesis, characterization and derivatization of some novel types of mono- and bis-imidazolidineiminothiones and imidazolidineiminodithiones with antitumor, antiviral, antibacterial and antifungal activities – part I, Eur. J. Med. Chem. 44 (2009) 4315–4334, https://doi.org/10.1016/j.ejmech.2009.07.019.
[13] P.G.C. de Carvalho, J.M. Ribeiro, G. Nakazato, R.P.B. Garbin, S.F.Y. Ogatta, Â. de Fátima, M.L.F. Bispo, F. Macedo Jr., Synthesis and antimicrobial activity of thiohydantoins derived from L-amino acids, Lett. Drug Des. Discov. 16 (2018), https://doi.org/10.2174/1570180816666181212153011.
[14] A. Buchynskyy, J.R. Gillespie, Z.M. Herbst, R.M. Ranade, F.S. Buckner, M.H. Gelb, 1-Benzyl-3-aryl-2-thiohydantoin derivatives as new anti- *Trypanosoma brucei* agents: SAR and in vivo efficacy, ACS Med. Chem. Lett. 8 (2017) 886–891, https://doi.org/10.1021/acsmedchemlett.7b00230.
[15] R. Raj, V. Mehra, J. Gut, P.J. Rosenthal, K.J. Wicht, T.J. Egan, M. Hopper, L. A. Wrischnik, K.M. Land, V. Kumar, Discovery of highly selective 7-chloroquinoline-thiohydantoins with potent antimalarial activity, Eur. J. Med. Chem. 84 (2014) 425–432, https://doi.org/10.1016/j.ejmech.2014.07.048.
[16] S. Porwal, S.S. Chauhan, P.M.S. Chauhan, N. Shakya, A. Verma, S. Gupta, Discovery of novel antileishmanial agents in an attempt to synthesize Pentamidine−Aplysinopsin hybrid molecule, J. Med. Chem. 52 (2009) 5793–5802, https://doi.org/10.1021/jm900564x.
[17] P.G. Camargo, B.T. da S. Bortoleti, M. Fabris, M.D. Gonçalves, F. Tomiotto-Pellissier, I.N. Costa, I. Conchon-Costa, C.H. da S. Lima, W.R. Pavanelli, M. de L. F. Bispo, F. Macedo, Thiohydantoins as anti-leishmanial agents: in vitro biological evaluation and multi-target investigation by molecular docking studies, J. Biomol. Struct. Dyn. (2020) 1–10, https://doi.org/10.1080/07391102.2020.1845979.
[18] P.G.C. de Carvalho, J.M. Ribeiro, R.P.B. Garbin, G. Nakazato, S.F. Yamada Ogatta, Â. de Fátima, M. de Lima Ferreira Bispo, F. Macedo, Synthesis and antimicrobial activity of thiohydantoins obtained from L-amino acids, Lett. Drug Des. Discov. 17 (2018) 94–102, https://doi.org/10.2174/1570180816666181212153011.
[19] F.M. Marim, T.N. Silveira, D.S. Lima, D.S. Zamboni, A method for generation of bone marrow-derived macrophages from cryopreserved mouse bone marrow cells, PLoS One 5 (2010), e15263, https://doi.org/10.1371/journal.pone.0015263.
[20] B.T. da S. Bortoleti, M.D. Gonçalves, F. Tomiotto-Pellissier, M.M. Miranda-Sapla, J. P. Assolini, A.C.M. Carloto, P.G.C. de Carvalho, I.L.A. Cardoso, A.N.C. Simão, N. S. Arakawa, I.N. Costa, I. Conchon-Costa, W.R. Pavanelli, Grandiflorenic acid promotes death of promastigotes via apoptosis-like mechanism and affects amastigotes by increasing total iron bound capacity, Phytomedicine 46 (2018) 11–20, https://doi.org/10.1016/j.phymed.2018.06.010.
[21] L.M.R. Antinarelli, I. de Oliveira Souza, P.V. Zabala Capriles, J. Gameiro, E. A. Britta, C.V. Nakamura, W.P. Lima, A.D. da Silva, E.S. Coimbra, Antileishmanial activity of a 4-hydrazinoquinoline derivative: induction of autophagy and apoptosis-related processes and effectiveness in experimental cutaneous leishmaniasis, Exp. Parasitol. 195 (2018) 78–86, https://doi.org/10.1016/j.exppara.2018.10.007.
[22] F. Tomiotto-Pellissier, D.R. Alves, M.M. Miranda-Sapla, S.M. de Morais, J. P. Assolini, B.T. da Silva Bortoleti, M.D. Gonçalves, A.H.D. Cataneo, D. Kian, T. B. Madeira, L.M. Yamauchi, S.L. Nixdorf, I.N. Costa, I. Conchon-Costa, W. R. Pavanelli, *Caryocar coriaceum* extracts exert leishmanicidal effect acting in promastigote forms by apoptosis-like mechanism and intracellular amastigotes by Nrf2/HO-1/ferritin dependent response and iron depletion, Biomed. Pharmacother. 98 (2018) 662–672, https://doi.org/10.1016/j.biopha.2017.12.083.
[23] P.H.F. Stroppa, L.M.R. Antinarelli, A.M.L. Carmo, J. Gameiro, E.S. Coimbra, A. D. da Silva, Effect of 1,2,3-triazole salts, non-classical bioisosteres of miltefosine, on *Leishmania amazonensis*, Bioorg. Med. Chem. 25 (2017) 3034–3045, https://doi.org/10.1016/j.bmc.2017.03.051.
[24] P. de A. Machado, J.O.F. Morais, G.S.G. Carvalho, W.P. Lima, G.C. Macedo, E. A. Britta, C.V. Nakamura, A.D. da Silva, A. Cuin, E.S. Coimbra, VOSalophen: a vanadium complex with a stilbene derivative—induction of apoptosis, autophagy, and efficiency in experimental cutaneous leishmaniasis, JBIC J. Biol. Inorg. Chem. 22 (2017) 929–939, https://doi.org/10.1007/s00775-017-1471-2.
[25] M.D. Gonçalves, B.T.S. Bortoleti, F. Tomiotto-Pellissier, M.M. Miranda-Sapla, J. P. Assolini, A.C.M. Carloto, P.G.C. Carvalho, E.T. Tudisco, A. Urbano, S. R. Ambrósio, E.Y. Hirooka, A.N.C. Simão, I.N. Costa, W.R. Pavanelli, I. Conchon-Costa, N.S. Arakawa, Dehydroabietic acid isolated from *Pinus elliottii* exerts in vitro antileishmanial action by pro-oxidant effect, inducing ROS production in promastigote and downregulating Nrf2/ferritin expression in amastigote forms of *Leishmania amazonensis*, Fitoterapia 128 (2018) 224–232, https://doi.org/10.1016/j.fitote.2018.05.027.
[26] C.A. Lipinski, Lead- and drug-like compounds: the rule-of-five revolution, Drug Discov. Today Technol. 1 (2004) 337–341, https://doi.org/10.1016/j.ddtec.2004.11.007.

[27] D.F. Veber, S.R. Johnson, H.-Y. Cheng, B.R. Smith, K.W. Ward, K.D. Kopple, Molecular properties that influence the oral bioavailability of drug candidates, J. Med. Chem. 45 (2002) 2615–2623, https://doi.org/10.1021/jm020017n.
[28] F. Cheng, W. Li, Y. Zhou, J. Shen, Z. Wu, G. Liu, P.W. Lee, Y. Tang, admetSAR: a comprehensive source and free Tool for assessment of chemical ADMET properties, J. Chem. Inf. Model. 52 (2012) 3099–3105, https://doi.org/10.1021/ci300367a.
[29] E.L. D'Antonio, B. Ullman, S.C. Roberts, U.G. Dixit, M.E. Wilson, Y. Hai, D. W. Christianson, Crystal structure of arginase from *Leishmania mexicana* and implications for the inhibition of polyamine biosynthesis in parasitic infections, Arch. Biochem. Biophys. 535 (2013) 163–176, https://doi.org/10.1016/j.abb.2013.03.015.
[30] D.A. Evans, History of the harvard ChemDraw project, Angew. Chem. Int. Ed. 53 (2014) 11140–11145, https://doi.org/10.1002/anie.201405820.
[31] O. Korb, T. Stützle, T.E. Exner, An ant colony optimization approach to flexible protein–ligand docking, Swarm Intell 1 (2007) 115–134, https://doi.org/10.1007/s11721-007-0006-9.
[32] S. Makeneni, D.F. Thieker, R.J. Woods, Applying pose clustering and MD simulations to eliminate false positives in molecular docking, J. Chem. Inf. Model. 58 (2018) 605–614, https://doi.org/10.1021/acs.jcim.7b00588.
[33] K.E. Hevener, W. Zhao, D.M. Ball, K. Babaoglu, J. Qi, S.W. White, R.E. Lee, Validation of molecular docking programs for virtual screening against dihydropteroate synthase, J. Chem. Inf. Model. 49 (2009) 444–460, https://doi.org/10.1021/ci800293n.
[34] T.B. Johnson, L.H. Chernoff, B.B. Treat Johnson, Hydantoins: synthesis of 5-thiohydantoins. https://pubs.acs.org/sharingguidelines, 1912.
[35] K.T. Andrews, G. Fisher, T.S. Skinner-Adams, Drug repurposing and human parasitic protozoan diseases, Int. J. Parasitol. Drugs Drug Resist. 4 (2014) 95, https://doi.org/10.1016/J.IJPDDR.2014.02.002.
[36] L.H. Freitas-Junior, E. Chatelain, H.A. Kim, J.L. Siqueira-Neto, Visceral leishmaniasis treatment: what do we have, what do we need and how to deliver it? Int. J. Parasitol. Drugs Drug Resist. 2 (2012) 11–19, https://doi.org/10.1016/j.ijpddr.2012.01.003.
[37] S. Cho, S.-H. Kim, D. Shin, Recent applications of hydantoin and thiohydantoin in medicinal chemistry, Eur. J. Med. Chem. 164 (2019) 517–545, https://doi.org/10.1016/J.EJMECH.2018.12.066.
[38] H. van de Waterbeemd, E. Gifford, ADMET in silico modelling: towards prediction paradise? Nat. Rev. Drug Discov. 2 (2003) 192–204, https://doi.org/10.1038/nrd1032.
[39] S.Q. Tang, Y.Y.I. Lee, D.S. Packiaraj, H.K. Ho, C.L.L. Chai, Systematic evaluation of the metabolism and toxicity of Thiazolidinone and imidazolidinone heterocycles, Chem. Res. Toxicol. 28 (2015) 2019–2033, https://doi.org/10.1021/acs.chemrestox.5b00247.
[40] E. Szymańska, K. Kieć-Kononowicz, Antimycobacterial activity of 5-arylidene aromatic derivatives of hydantoin, Farm 57 (2002) 355–362, https://doi.org/10.1016/S0014-827X(01)01194-6.
[41] R.J. Wheeler, E. Gluenz, K. Gull, The cell cycle of Leishmania: morphogenetic events and their implications for parasite biology, Mol. Microbiol. 79 (2011) 647–662, https://doi.org/10.1111/j.1365-2958.2010.07479.x.
[42] A. Ambit, K.L. Woods, B. Cull, G.H. Coombs, J.C. Mottram, Morphological events during the cell cycle of *Leishmania major*, Eukaryot. Cell 10 (2011) 1429–1438, https://doi.org/10.1128/EC.05118-11.
[43] M.S. da Silva, J.P. Monteiro, V.S. Nunes, E.J. Vasconcelos, A.M. Perez, L. de H. Freitas-Júnior, M.C. Elias, M.I.N. Cano, *Leishmania amazonensis* promastigotes present two Distinct modes of nucleus and kinetoplast segregation during cell cycle, PLoS One 8 (2013), e81397, https://doi.org/10.1371/journal.pone.0081397.
[44] W.R. Proto, G.H. Coombs, J.C. Mottram, Cell death in parasitic protozoa: regulated or incidental? Nat. Rev. Microbiol. 11 (2013) 58–66, https://doi.org/10.1038/nrmicro2929.
[45] I.S. Chauhan, G.S. Rao, J. Shankar, L.K.S. Chauhan, G.J. Kapadia, N. Singh, Chemoprevention of Leishmaniasis: in-vitro antiparasitic activity of dibenzalacetone, a synthetic curcumin analog leads to apoptotic cell death in *Leishmania donovani*, Parasitol. Int. 67 (2018) 627–636, https://doi.org/10.1016/j.parint.2018.06.004.
[46] M.K. Singh, S.K. Bhaumik, S. Karmakar, J. Paul, S. Sawoo, H.K. Majumder, A. Roy, Copper salisylaldoxime (CuSAL) imparts protective efficacy against visceral leishmaniasis by targeting *Leishmania donovani* topoisomerase IB, Exp. Parasitol. 175 (2017) 8–20, https://doi.org/10.1016/j.exppara.2017.02.010.
[47] B.T. da S. Bortoleti, F. Tomiotto-Pellissier, M.D. Gonçalves, M.M. Miranda-Sapla, J. P. Assolini, A.C. Carloto, D.M. Lima, G.F. Silveira, R.S. Almeida, I.N. Costa, I. Conchon-Costa, W.R. Pavanelli, Caffeic acid has antipromastigote activity by apoptosis-like process; and anti-amastigote by TNF-α/ROS/NO production and decreased of iron availability, Phytomedicine 57 (2019) 262–270, https://doi.org/10.1016/j.phymed.2018.12.035.
[48] R.F.S. Menna-Barreto, Cell death pathways in pathogenic trypanosomatids: lessons of (over)kill, Cell Death Dis. 10 (2019) 93, https://doi.org/10.1038/s41419-019-1370-2.
[49] D. Smirlis, M. Duszenko, A. Ruiz, E. Scoulica, P. Bastien, N. Fasel, K. Soteriadou, Targeting essential pathways in trypanosomatids gives insights into protozoan mechanisms of cell death, Parasites Vectors 3 (2010) 107, https://doi.org/10.1186/1756-3305-3-107.
[50] S.-J. Lee, J. Zhang, A.M.K. Choi, H.P. Kim, Mitochondrial dysfunction induces formation of lipid droplets as a generalized response to stress, Oxid. Med. Cell. Longev. 2013 (2013) 327167, https://doi.org/10.1155/2013/327167.
[51] H. Volpato, V.C. Desoti, R.H. Valdez, T. Ueda-Nakamura, S. de O. Silva, M. H. Sarragiotto, C.V. Nakamura, Mitochondrial dysfunction induced by N-Butyl-1-(4-Dimethylamino)Phenyl-1,2,3,4-Tetrahydro-β-Carboline-3-Carboxamide is required for cell death of *Trypanosoma cruzi*, PLoS One 10 (2015), e0130652, https://doi.org/10.1371/journal.pone.0130652.
[52] J. Boren, K.M. Brindle, Apoptosis-induced mitochondrial dysfunction causes cytoplasmic lipid droplet formation, Cell Death Differ. 19 (2012) 1561–1570, https://doi.org/10.1038/cdd.2012.34.
[53] A. Brennand, E. Rico, P.A.M. Michels, Autophagy in trypanosomatids, Cells 1 (2012) 346–371, https://doi.org/10.3390/cells1030346.
[54] S. Dolai, S. Adak, Endoplasmic reticulum stress responses in Leishmania, Mol. Biochem. Parasitol. 197 (2014) 1–8, https://doi.org/10.1016/j.molbiopara.2014.09.002.
[55] D.O. dos Anjos, E.S. Sobral Alves, V.T. Gonçalves, S.S. Fontes, M.L. Nogueira, A. M. Suarez-Fontes, J.B. Neves da Costa, F. Rios-Santos, M.A. Vannier-Santos, Effects of a novel β–lapachone derivative on *Trypanosoma cruzi*: parasite death involving apoptosis, autophagy and necrosis, Int. J. Parasitol. Drugs Drug Resist. 6 (2016) 207–219, https://doi.org/10.1016/j.ijpddr.2016.10.003.
[56] E. Valdivieso, F. Mejías, C. Torrealba, G. Benaim, V.V. Kouznetsov, F. Sojo, F. A. Rojas-Ruiz, F. Arvelo, F. Dagger, In vitro 4-Aryloxy-7-chloroquinoline derivatives are effective in mono- and combined therapy against *Leishmania donovani* and induce mitocondrial membrane potential disruption, Acta Trop. 183 (2018) 36–42, https://doi.org/10.1016/j.actatropica.2018.03.023.
[57] M. Ortalli, S. Varani, C. Rosso, A. Quintavalla, M. Lombardo, C. Trombini, Evaluation of synthetic substituted 1,2-dioxanes as novel agents against human leishmaniasis, Eur. J. Med. Chem. 170 (2019) 126–140, https://doi.org/10.1016/j.ejmech.2019.02.070.
[58] P.P. Carneiro, J. Conceição, M. Macedo, V. Magalhães, E.M. Carvalho, O. Bacellar, The role of nitric oxide and reactive oxygen species in the killing of *Leishmania braziliensis* by monocytes from patients with cutaneous leishmaniasis, PLoS One 11 (2016), https://doi.org/10.1371/journal.pone.0148084.
[59] C.N. Paiva, M.T. Bozza, Are reactive oxygen species always detrimental to pathogens? Antioxidants Redox Signal. 20 (2014) 1000–1034, https://doi.org/10.1089/ars.2013.5447.
[60] S. Nylén, S. Gautam, Immunological perspectives of leishmaniasis, J. Global Infect. Dis. 2 (2010) 135, https://doi.org/10.4103/0974-777x.62876.
[61] N.W. Andrews, Oxidative stress and intracellular infections: more iron to the fire, J. Clin. Invest. 122 (2012) 2352–2354, https://doi.org/10.1172/JCI64239.
[62] P. Cecílio, B. Pérez-Cabezas, N. Santarém, J. Maciel, V. Rodrigues, A.C. da Silva, Deception and manipulation: the arms of Leishmania, a successful parasite, Front. Immunol. 5 (2014), https://doi.org/10.3389/fimmu.2014.00480.
[63] W. Yu, Z. Guo, P. Orth, V. Madison, L. Chen, C. Dai, R.J. Feltz, V. M. Girijavallabhan, S.H. Kim, J.A. Kozlowski, B.J. Lavey, D. Li, D. Lundell, X. Niu, J.J. Piwinski, J. Popovici-Muller, R. Rizvi, K.E. Rosner, B.B. Shankar, N.Y. Shih, M. Arshad Siddiqui, J. Sun, L. Tong, S. Umland, M.K.C. Wong, D. yi Yang, G. Zhou, Discovery and SAR of hydantoin TACE inhibitors, Bioorg. Med. Chem. Lett 20 (2010) 1877–1880, https://doi.org/10.1016/j.bmcl.2010.01.148.
[64] L. Tong, S.H. Kim, K. Rosner, W. Yu, B.B. Shankar, L. Chen, D. Li, C. Dai, V. Girijavallabhan, J. Popovici-Muller, L. Yang, G. Zhou, A. Kosinski, M. A. Siddiqui, N.Y. Shih, Z. Guo, P. Orth, S. Chen, D. Lundell, X. Niu, S. Umland, J. A. Kozlowski, Fused bi-heteroaryl substituted hydantoin compounds as TACE inhibitors, Bioorg. Med. Chem. Lett 27 (2017) 3037–3042, https://doi.org/10.1016/j.bmcl.2017.05.062.